Table 2 IC_{50} values(μM) of CDDP and NC-6004 in various cancer cell lines

		Exposure time (h)			
		48		72	
Cancer	Cell line	CDDP	NC-6004	CDDP	NC-6004
Bladder cancer	EJ-1	2.46	25.45	1.86	18.44
	J82	2.78	42.89	2.42	20.27
	MBT-2	15.88	>100	5.67	71.67
Colon cancer	Colo201	34.77	>100	28.52	>100
	Colo320	16.32	>100	9.71	81.15
	HT-29	14.44	>100	8.83	>100
Lung cancer	A549	21.43	>100	20	>100
	EBC-1	>100	>100	9.36	84.78
	PC-14	16.81	>100	8.73	87.11
Gastric cancer	MKN-28	>100	>100	8.23	76.81
	MKN-45	7.12	68.36	6.94	43.81
Breast cancer	MCF-7	12.78	>100	5.71	54.71

the CDDP 5 mg kg^{-1} administration group showed a significant decrease ($P<0.01$) in tumour growth rate as compared with the control group. In the administration of NC-6004, NC-6004 2.5 mg kg^{-1} administration group ($P<0.05$) and 5 mg kg^{-1} administration group ($P<0.01$) showed significant decreases in tumour growth rate as compared with the control group. However, the NC-6004 administration groups at the same dose levels as CDDP showed no significant difference in tumour growth rate. The same animal model was used to repeat the study using the drugs at different dose levels, and similar tendencies were observed (data not shown). Regarding time-course changes in body weight change rate, the CDDP 5 mg kg^{-1} administration group showed a significant decrease ($P<0.001$) in body weight as compared with the control group. On the other hand, none of the NC-6004 administration groups showed a decrease in body weight as compared with the control group (Figure 3B).

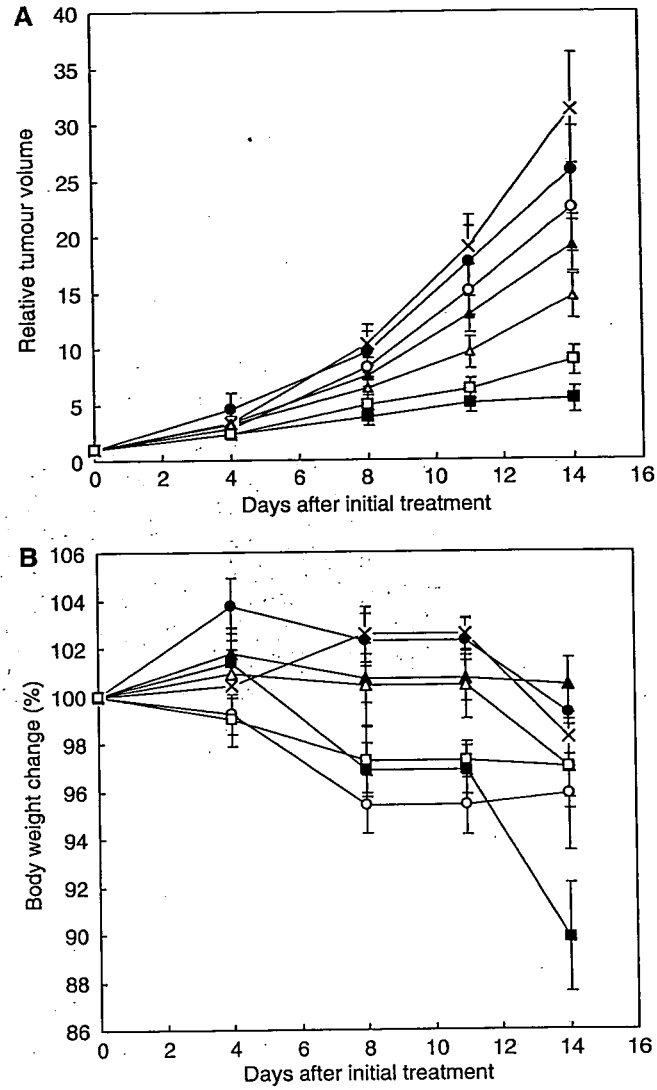

Figure 3 Relative changes in MKN-45 tumour growth rates in nude mice. (**A**) Cisplatin and NC-6004 were injected i.v. every 3 days, three administrations in total, at CDDP-equivalent doses of 0.5 mg kg^{-1} (●, ○), 2.5 mg kg^{-1} (▲, △), and 5 mg kg^{-1} (■, □), respectively. Glucose (5%) was injected in the control mice (×). (**B**) Changes in relative body weight. Data were derived from the same mice as those used in the present study. Values are expressed as the mean±s.e.

Nephrotoxicity and hepatotoxicity of CDDP and NC-6004

In the CDDP 10 mg kg^{-1} administration group, four of 12 animals died from toxicity within 7 days after drug administration. No deaths occurred in the NC-6004 10 mg kg^{-1} administration group and the NC-6004 15 mg kg^{-1} administration group. Regarding renal function, the BUN concentrations on day 7 after the administration of 5% glucose, CDDP 10 mg kg^{-1}, NC-6004 10 mg kg^{-1}, and NC-6004 15 mg kg^{-1} were 20.8±3.0, 65.3±44.4, 20±4.5, and 24.6±18.2 mg dl^{-1}, respectively. The plasma concentrations of creatinine on day 7 after the administration of 5% glucose, CDDP 10 mg kg^{-1}, NC-6004 10 mg kg^{-1}, and NC-6004 15 mg kg^{-1} were 0.27±0.03, 0.68±0.23, 0.28±0.04, and 0.45±0.11 mg dl^{-1}, respectively. The CDDP 10 mg kg^{-1} administration group showed significantly higher plasma concentrations of BUN and creatinine as compared with the control group ($P<0.05$ and 0.001, respectively), with the NC-6004 10 mg kg^{-1} administration group ($P<0.05$ and 0.001, respectively), and also with the NC-6004 15 mg kg^{-1} administration group ($P<0.05$ and 0.05, respectively) (Figure 4A and B). Light microscopy indicated tubular dilation with flattening of the lining cells of the tubular epithelium in the kidney from all animals in the CDDP 10 mg kg^{-1} administration group. On the other hand, no histopathological change was observed in the kidneys from all animals in the NC-6004 10 mg kg^{-1} administration group (Figure 4C and D). Regarding hepatic function, the plasma concentrations of GOT on day 7 after the administration of 5% glucose, CDDP 10 mg kg^{-1}, NC-6004 10 mg kg^{-1}, and NC-6004 15 mg kg^{-1} were 68±6.8, 65.1±5.5, 106±13.1, and 97±16.2 IU l^{-1}, respectively. The plasma concentrations of GPT on day 7 after the administration of 5% glucose, CDDP 10 mg kg^{-1}, NC-6004 10 mg kg^{-1}, and NC-6004 15 mg kg^{-1} were 39.6±10, 32±6.4, 92±18.9, and 55±11.3 IU l^{-1}, respectively. The CDDP 10 mg kg^{-1} administration group showed plasma concentrations of GOT and GPT which were comparable to those in the control group. However, the NC-6004 10 mg kg^{-1} administration group, which presented the same dose level as the CDDP 10 mg kg^{-1} administration group, showed significantly higher plasma concentrations of GOT and GPT ($P<0.001$ and 0.01, respectively) as compared with the control group. Furthermore, the NC-6004 15 mg kg^{-1} administration group also showed significantly higher plasma concentrations of GOT ($P<0.001$) as compared with the control group. However, the plasma concentrations of GOT and GPT on day 14 after the administration of NC-6004 10 mg kg^{-1} were comparable to those in the control group (74±2.3 and 42.8±5.1 IU l^{-1}, respectively) (Figure 4E). These results lead to the conjecture that rats which were given NC-6004 10 mg kg^{-1}, i.v., showed transient and reversible hepatotoxicity.

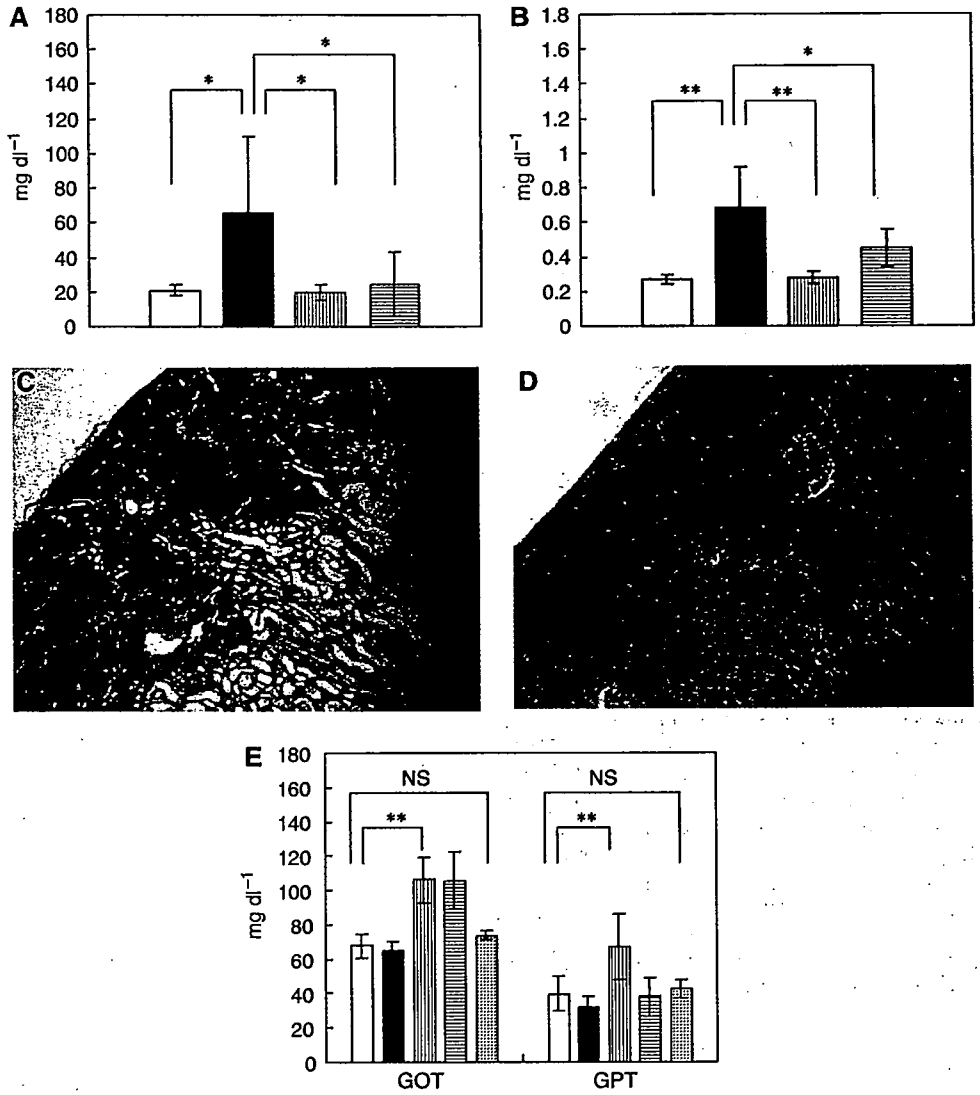

Figure 4 Nephrotoxicity and hepatotoxicity of CDDP and NC-6004. Plasma concentrations of BUN (**A**) and creatinine (**B**) were measured after a single i.v. injection of 5% glucose (□) ($n=8$), CDDP at a dose of 10 mg kg^{-1} (■) ($n=12$), NC-6004 at a dose of 10 mg kg^{-1} ($n=13$) on a CDDP basis (▥), and at a dose of 15 mg kg^{-1} on a CDDP basis (▤) ($n=8$) to rats. Histopathological changes in the kidney on day 7 after the i.v. injection of CDDP (**C**, ×4) and NC-6004 (**D**, ×4) in rats at an equivalent dose of 10 mg kg^{-1} CDDP. In rats given CDDP, widespread tubular degeneration as indicated by tubular dilation with flattening of the lining cells of tubular epithelium was seen. On the other hand, no histopathological change was observed in the kidney from all animals in the NC-6004 10 mg kg^{-1} administration group. For hepatotoxicity (**E**), the plasma concentrations of GOT and GPT were measured on day 7 after administration. When administering NC-6004 at a dose of 10 mg kg^{-1} on a CDDP basis, five of 13 blood samples were taken on day 14 after administration (▦). The other samples were taken on day 7 administration. In the group given CDDP at a dose of 10 mg kg^{-1}, four of 12 rats died within 7 days. Values are expressed as the mean ± s.d. *$P<0.05$, **$P<0.001$, NS: not significant.

Neurotoxicity of CDDP and NC-6004

Neurophysiological examination revealed that MNCVs in animals given 5% glucose, CDDP, and NC-6004 were 44.2±3.5, 40.94±5.08, and 40.62±0.63 m s^{-1}, respectively. No significant difference was found among the groups with respect to MNCV. Furthermore, SNCVs in animals given 5% glucose, CDDP, and NC-6004 were 42.86±8.07, 35.48±4.91, and 43.74±5.3 m s^{-1}, respectively. Animals given NC-6004 showed no delay in SNCV as compared with animals given 5% glucose. On the other hand, animals given CDDP showed a significant delay ($P<0.05$) in SNCV as compared with animals given NC-6004 (Figure 5A). In addition, histopathological examination with electron microscopy revealed degenerations, as manifested by electron photomicrographs indicating degenerative changes, for example, loss of microtubules, degeneration in the cytoplasm of Schwann cells, loss of filaments, and an irregular inner loop, in approximately 80% of myelinated segments of the sciatic nerve from animals given CDDP. On the other hand, animals given NC-6004 exhibited nearly normal electron photomicrographs of the sciatic nerve as the control animals did (Figure 5B and C). These results indicate that NC-6004 reduced peripheral neurotoxicity as compared with CDDP. Furthermore, regarding body weight change as an indication of general toxicity, furthermore, the NC-6004 administration groups showed significant inhibition of body weight decrease ($P<0.001$) as compared with the CDDP administration group ($P<0.001$) (Figure 5D).

The analysis by ICP-MS on sciatic nerve concentrations of Pt could not detect Pt in the sciatic nerve from animals given 5% glucose (data not shown). Sciatic nerve concentrations of Pt in

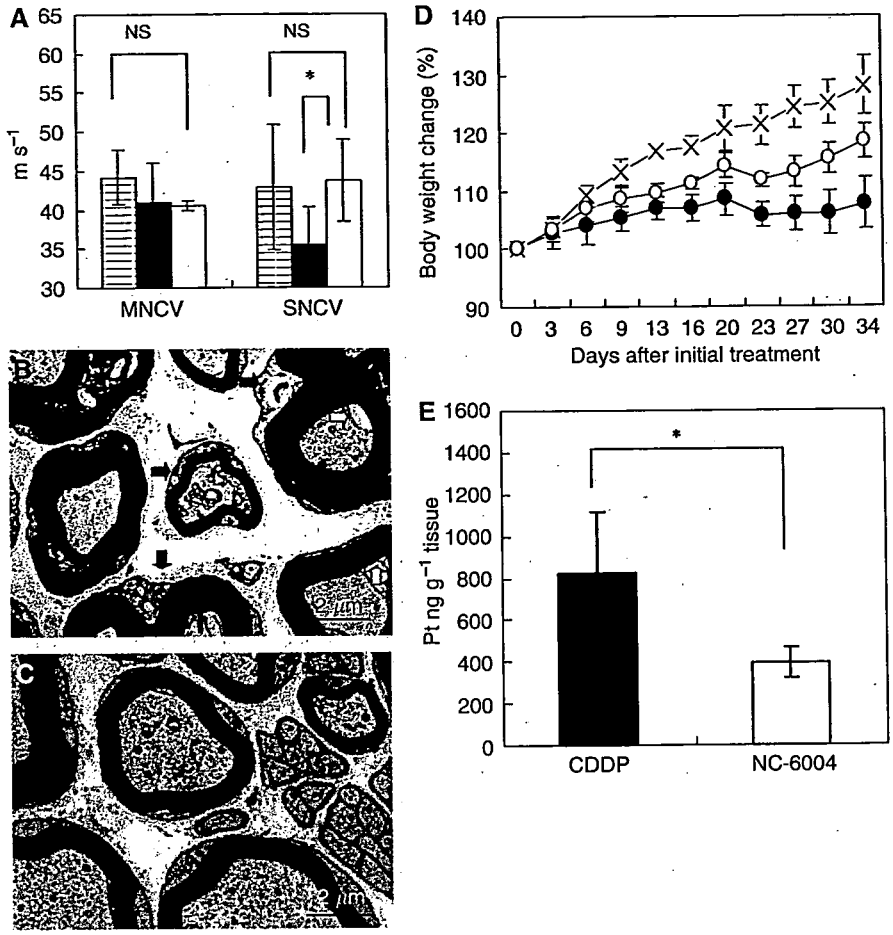

Figure 5 Neurotoxicity of CDDP and NC-6004 in rats. Rats ($n=5$) were given CDDP (2 mg kg^{-1}), NC-6004 (an equivalent dose of 2 mg kg^{-1} CDDP), or 5% glucose, all i.v. twice a week, 11 administrations in total. (**A**) Sensory nerve conduction velocity and MNCV of the sciatic nerve at week 6 after the initial administration (control (⊟), CDDP (●), and NC-6004 (□)). Histopathological changes of the sciatic nerve were examined by electron microscopy after the administration of CDDP (**B**) and NC-6004 (**C**). In rats given CDDP, widespread degenerations as indicated by loss of microtubules, loss of filaments, degeneration in the cytoplasm of Schwann cells (➡), and an irregular inner loop (⇨) were seen. On the other hand, animals given NC-6004 exhibited nearly normal electron micrographs of the sciatic nerve as the control animals. (**D**) Changes in relative body weight. Data were derived from the same rats as those used in the present study (control (×), CDDP (●), and NC-6004 (○)). (**E**) The Pt concentration in the sciatic nerve. Rats were given CDDP (■) (5 mg kg^{-1}, $n=5$), NC-6004 (□) (an equivalent dose of 5 mg kg^{-1} CDDP, $n=5$), or 5% glucose ($n=2$), all i.v. twice a week, four administrations in total. On day 3 after the final administration, a segment of the sciatic nerve was removed and the Pt concentration in the sciatic nerve was measured by ICP-MS. Body weight changes are expressed as the mean ± s.e. The other data are expressed as the mean ± s.d. *$P<0.05$, **$P<0.001$, NS: not significant.

animals given CDDP and NC-6004 were 827.2 ± 291.3 and 395.5 ± 73.1 ng g^{-1} tissue. Therefore, the concentrations were significantly ($P<0.05$) lower in animals given NC-6004 (Figure 5E). This finding is believed to be a factor which reduced neurotoxicity following NC-6004 administration as compared with the CDDP administration.

DISCUSSION

The present study indicated that CDDP-incorporating polymeric micelles (NC-6004) are stable nanoparticles with a long blood retention profile as compared with free CDDP. NC-6004 showed 6- to 15-fold less potent *in vitro* cytotoxic activity in several human cancer cell lines as compared with CDDP. These findings are considered attributable to the slow release of free CDDP in the presence of abundant chloride ions because NC-6004 contains coordination bonds between the atoms of Pt(II) of CDDP and the carboxylic group in the side chain of P(Glu). *In vivo*, however, in contrast to the *in vitro* findings, NC-6004 was found to markedly reduce nephrotoxicity and neurotoxicity – dose-limiting factors of CDDP, while preserving antitumour activity, which was equivalent to or better than that of free CDDP.

Nephrotoxicity of CDDP is considered to depend on the peak urinary CDDP concentration and on the maximum CDDP concentration in the uriniferous tubules (Levi *et al*, 1982). We consider that the reduced nephrotoxicity of NC-6004 may be explained by the following facts: (1) the tendency of micelles to be less prone to filtration by nephrons because of the NC-6004 particle size (approximately 30 nm), and (2) the much lower C_{max} value for CDDP at least in the uriniferous tubules than the value following CDDP administration. NC-6004 possibly facilitates treatment on an outpatient basis because it allows safer administration to patients with decreased renal function and requires no massive fluid replacement to protect renal tissue after the administration of CDDP.

The main neuropathy of CDDP is sensory peripheral neuropathy (van der Hoop *et al*, 1990; Gregg *et al*, 1992). A delay in SNCV due to the injury of dorsal root ganglia and peripheral nerve has previously been reported in rats given CDDP, although MNCV was

preserved in the tail and hind paws of rats (McKeage *et al*, 1994; Tredici *et al*, 1998; Meijer *et al*, 1999; Tredici *et al*, 1999). Furthermore, histopathological examination revealed degenerative changes in the sciatic nerve in similar experimental animals (Cavaletti *et al*, 1992; Tredici *et al*, 1999). In the present study, animals given NC-6004 showed no delay in the SNCV, while animals given CDDP showed a significant delay in the SNCV as compared with animals given NC-6004. Neuropathologically, neuronal degeneration, which was observed following CDDP administration, was not observed with NC-6004 administration. This result is considered attributable principally to the fact that the peripheral nerve concentration of Pt decreased to half or less following NC-6004 administration than with CDDP administration. The nervous tissue concentration of Pt at the time of NC-6004 administration decreased significantly despite the fact that the plasma AUC at the time of NC-6004 administration was high, being 65-fold higher than the plasma AUC concentration with CDDP administration. We consider that this result is attributed to the marked inhibition of Pt distribution into nervous tissue in the NC-6004 administration groups as manifested by V_{ss} of 3.00 ± 0.61 and $0.04 \pm 0.0023\,l\,kg^{-1}$ in the CDDP and NC-6004 groups, respectively. In any event, we believe that the neurotoxicity of CDDP reduced by NC-6004 allows its long-term administration.

On the other hand, transient hepatic dysfunction was observed in rats. This observation indicates the proneness of Pt to accumulate in the RES of the liver because NC-6004 is, after all, said and done, a macromolecule, although preserving a stealth effect through its outer shell of PEG. We consider that caution should be exercised against hepatic dysfunction in conducting a clinical trial of NC-6004 in the future. However, the accumulation of Pt was lower following NC-6004 administration due to a decrease in V_{ss} in other organs including nerve. As shown by changes in body weight in multiple dose studies in rats, the NC-6004 administration groups have been demonstrated to show a smaller decrease in body weight as compared with the CDDP administration groups. In single-dose studies, furthermore, one dose of CDDP $10\,mg\,kg^{-1}$ was equivalent to the 50% of the lethal dose. In fact, four of 12 animals died within 7 days after administration. However, none of the eight animals in the NC-6004 group died after the administration of NC-6004 at a CDDP equivalent dose of $15\,mg\,kg^{-1}$. In terms of haematological toxicity, there was no significant difference between the CDDP and NC-6004 groups in rats (data not shown).

In murine tumour strains, CDDP-incorporating polymeric micelles showed significantly high antitumour activity (Nishiyama *et al*, 2003). In the human gastric cancer strain used in the present study, however, no significant difference was found between the NC-6004 and CDDP administration groups. A significant difference was found in antitumour activity between the NC-6004 low-dose group ($2.5\,mg\,kg^{-1}$ administration group) and the control group, while no significant difference was found between the CDDP low-dose group ($2.5\,mg\,kg^{-1}$ administration group) and the control group. Results available to date and the results from the present study lead to the consideration that the incorporation of CDDP into polymeric micelles does not reduce its antitumour activity.

Data from the present study warrant the clinical evaluation of NC-6004. We consider that the protocol for the Phase I clinical trial of NC-6004 should employ a regimen without massive i.v. drip infusion.

Translational Therapeutics

ACKNOWLEDGEMENTS

This work is supported by Grants-in-Aid from the Ministry of Health, Labour and Welfare of Japan. We thank Drs T Kawaguchi and K Shimada for their expert technical assistance and Mrs K Shiina for her secretarial assistance.

REFERENCES

Allen TM (1994) Long-circulating (sterically stabilized) liposomes for targeted drug delivery. *Trends Pharmacol Sci* 15: 215–220

Bellmunt J, Ribas A, Eres N, Albanell J, Almanza C, Bermejo B, Sole LA, Baselga J (1997) Carboplatin-based *versus* cisplatin-based chemotherapy in the treatment of surgically incurable advanced bladder carcinoma. *Cancer* 80: 1966–1972

Boulikas T, Vougiouka M (2004) Recent clinical trials using cisplatin, carboplatin and their combination chemotherapy drugs (review). *Oncol Rep* 11: 559–595

Cassidy J, Tabernero J, Twelves C, Brunet R, Butts C, Conroy T, Debraud F, Figer A, Grossmann J, Sawada N, Schoffski P, Sobrero A, Van Cutsem E, Diaz-Rubio E (2004) XELOX (capecitabine plus oxaliplatin): active first-line therapy for patients with metastatic colorectal cancer. *J Clin Oncol* 22: 2084–2091

Cavaletti G, Tredici G, Marmiroli P, Petruccioli MG, Barajon I, Fabbrica D (1992) Morphometric study of the sensory neuron and peripheral nerve changes induced by chronic cisplatin (DDP) administration in rats. *Acta Neuropathol (Berl)* 84: 364–371

Cleare MJ, Hydes PC, Malerbi BW, Watkins DM (1978) Anti-tumor platinum complexes: relationships between chemical properties and activity. *Biochimie* 60: 835–850

du Bois A, Luck HJ, Meier W, Adams HP, Mobus V, Costa S, Bauknecht T, Richter B, Warm M, Schroder W, Olbricht S, Nitz U, Jackisch C, Emons G, Wagner U, Kuhn W, Pfisterer J (2003) A randomized clinical trial of cisplatin/paclitaxel *versus* carboplatin/paclitaxel as first-line treatment of ovarian cancer. *J Natl Cancer Inst* 95: 1320–1329

Gabizon A, Chemla M, Tzemach D, Horowitz AT, Goren D (1996) Liposome longevity and stability in circulation: effects on the *in vivo* delivery to tumors and therapeutic efficacy of encapsulated anthracyclines. *J Drug Target* 3: 391–398

Gregg RW, Molepo JM, Monpetit VJ, Mikael NZ, Redmond D, Gadia M, Stewart DJ (1992) Cisplatin neurotoxicity: the relationship between dosage, time, and platinum concentration in neurologic tissues, and morphologic evidence of toxicity. *J Clin Oncol* 10: 795–803

Hamaguchi T, Matsumura Y, Suzuki M, Shimizu K, Goda R, Nakamura I, Nakatomi I, Yokoyama M, Kataoka K, Kakizoe T (2005) NK105, a paclitaxel-incorporating micellar nanoparticle formulation, can extend *in vivo* antitumour activity and reduce the neurotoxicity of paclitaxel. *Br J Cancer* 92: 1240–1246

Horwich A, Sleijfer DT, Fossa SD, Kaye SB, Oliver RT, Cullen MH, Mead GM, de Wit R, de Mulder PH, Dearnaley DP, Cook PA, Sylvester RJ, Stenning SP (1997) Randomized trial of bleomycin, etoposide, and cisplatin compared with bleomycin, etoposide, and carboplatin in good-prognosis metastatic nonseminomatous germ cell cancer: a Multiinstitutional Medical Research Council/European Organization for Research and Treatment of Cancer Trial. *J Clin Oncol* 15: 1844–1852

Klibanov AL, Maruyama K, Beckerleg AM, Torchilin VP, Huang L (1991) Activity of amphipathic poly(ethylene glycol) 5000 to prolong the circulation time of liposomes depends on the liposome size and is unfavorable for immunoliposome binding to target. *Biochim Biophys Acta* 1062: 142–148

Klibanov AL, Maruyama K, Torchilin VP, Huang L (1990) Amphipathic polyethylene glycols effectively prolong the circulation time of liposomes. *FEBS Lett* 268: 235–237

Lasic DD (1996) Doxorubicin in sterically stabilized liposomes. *Nature* 380: 561–562

Levi FA, Hrushesky WJ, Halberg F, Langevin TR, Haus E, Kennedy BJ (1982) Lethal nephrotoxicity and hematologic toxicity of *cis*-diammine-dichloroplatinum ameliorated by optimal circadian timing and hydration. *Eur J Cancer Clin Oncol* 18: 471–477

Maeda H (2001) The enhanced permeability and retention (EPR) effect in tumor vasculature: the key role of tumor-selective macromolecular drug targeting. *Adv Enzyme Regul* 41: 189–207

Maeda H, Matsumura Y (1989) Tumoritropic and lymphotropic principles of macromolecular drugs. *Crit Rev Ther Drug Carrier Syst* 6: 193–210

Maeda H, Wu J, Sawa T, Matsumura Y, Hori K (2000) Tumor vascular permeability and the EPR effect in macromolecular therapeutics: a review. *J Control Rel* 65: 271–284

Matsumura Y, Hamaguchi T, Ura T, Muro K, Yamada Y, Shimada Y, Shirao K, Okusaka T, Ueno H, Ikeda M, Watanabe N (2004) Phase I clinical trial and pharmacokinetic evaluation of NK911, a micelle-encapsulated doxorubicin. *Br J Cancer* 91: 1775–1781

Matsumura Y, Maeda H (1986) A new concept for macromolecular therapeutics in cancer chemotherapy: mechanism of tumoritropic accumulation of proteins and the antitumor agent smancs. *Cancer Res* 46: 6387–6392

McKeage MJ, Boxall FE, Jones M, Harrap KR (1994) Lack of neurotoxicity of oral bisacetatoammine*dichlorocyclohexylamine-platinum(IV) in comparison to cisplatin and tetraplatin in the rat. *Cancer Res* 54: 629–631

Meijer C, de Vries EG, Marmiroli P, Tredici G, Frattola L, Cavaletti G (1999) Cisplatin-induced DNA-platination in experimental dorsal root ganglia neuronopathy. *Neurotoxicology* 20(6): 883–887

Nishiyama N, Kataoka K (2001) Preparation and characterization of size-controlled polymeric micelle containing *cis*-dichlorodiammineplatinum(II) in the core. *J Control Rel* 74: 83–94

Nishiyama N, Kato Y, Sugiyama Y, Kataoka K (2001) Cisplatin-loaded polymer–metal complex micelle with time-modulated decaying property as a novel drug delivery system. *Pharm Res* 18: 1035–1041

Nishiyama N, Okazaki S, Cabral H, Miyamoto M, Kato Y, Sugiyama Y, Nishio K, Matsumura Y, Kataoka K (2003) Novel cisplatin-incorporated polymeric micelles can eradicate solid tumors in mice. *Cancer Res* 63: 8977–8983

Nishiyama N, Yokoyama M, Aoyagi T, Okano T, Sakurai Y, Kataoka K (1999) Preparation and characterization of self-assembled polymer–metal complex micelle from *cis*-dichlorodiammineplatinum(II) and poly(ethylene glycol)-poly(α,β-aspartic acid) block copolymer in an aqueous medium. *Langmuir* 15: 377–383

Orditura M, Quaglia F, Morgillo F, Martinelli E, Lieto E, De Rosa G, Comunale D, Diadema MR, Ciardiello F, Catalano G, De Vita F (2004) Pegylated liposomal doxorubicin: pharmacologic and clinical evidence of potent antitumor activity with reduced anthracycline-induced cardiotoxicity (review). *Oncol Rep* 12: 549–556

Pinzani V, Bressolle F, Haug IJ, Galtier M, Blayac JP, Balmes P (1994) Cisplatin-induced renal toxicity and toxicity-modulating strategies: a review. *Cancer Chemother Pharmacol* 35: 1–9

Roth BJ (1996) Chemotherapy for advanced bladder cancer. *Semin Oncol* 23: 633–644

Screnci D, McKeage MJ, Galettis P, Hambley TW, Palmer BD, Baguley BC (2000) Relationships between hydrophobicity, reactivity, accumulation and peripheral nerve toxicity of a series of platinum drugs. *Br J Cancer* 82: 966–972

Tredici G, Braga M, Nicolini G, Miloso M, Marmiroli P, Schenone A, Nobbio L, Frattola L, Cavaletti G (1999) Effect of recombinant human nerve growth factor on cisplatin neurotoxicity in rats. *Exp Neurol* 159: 551–558

Tredici G, Tredici S, Fabbrica D, Minoia C, Cavaletti G (1998) Experimental cisplatin neuronopathy in rats and the effect of retinoic acid administration. *J Neurooncol* 36: 31–40

van der Hoop RG, van der Burg ME, ten Bokkel Huinink WW, van Houwelingen C, Neijt JP (1990) Incidence of neuropathy in 395 patients with ovarian cancer treated with or without cisplatin. *Cancer* 66: 1697–1702

UKCCCR, PO Box 123, Kincolin's Inn Fields, London, WC2A 3PX (1998) United Kingdom Co-ordinating Committee on Cancer Research (UKCCCR) guidelines for the welfare of animals in experimental neoplasia (second edition). *Br J Cancer* 77: 1–10

Yokoyama M, Miyauchi M, Yamada N, Okano T, Sakurai Y, Kataoka K, Inoue S (1990) Characterization and anticancer activity of the micelle-forming polymeric anticancer drug adriamycin-conjugated poly(ethylene glycol)-poly(aspartic acid) block copolymer. *Cancer Res* 50: 1693–1700

Yokoyama M, Okano T, Sakurai Y, Ekimoto H, Shibazaki C, Kataoka K (1991) Toxicity and antitumor activity against solid tumors of micelle-forming polymeric anticancer drug and its extremely long circulation in blood. *Cancer Res* 51: 3229–3236

Yokoyama M, Okano T, Sakurai Y, Fukushima S, Okamoto K, Kataoka K (1999) Selective delivery of adriamycin to a solid tumor using a polymeric micelle carrier system. *J Drug Target* 7: 171–186

Differential Cytotoxicity of Anticancer Agents in Pre- and Post-Immortal Lymphoblastoid Cell Lines

Kaori SAWADA, Keisuke NODA, Hiroto NAKAJIMA, Naoki SHIMBARA, Yasuhiro FURUICHI, and Masanobu SUGIMOTO*

GeneCare (previously AGENE) Research Institute; 200 Kajiwara, Kamakura, Kanagawa 247–0063, Japan.
Received January 31, 2005; accepted April 4, 2005

We studied the cytotoxic effect of various anticancer agents on lymphoblastoid cell lines transformed by Epstein–Barr virus. Post-immortal N0005 (post-N0005) is an immortalized cell line derived from pre-immortal N0005 (pre-N0005) accompanied by increased telomerase activity, short-telomere, abnormal karyotypes, mutation of *p53* gene, down regulation of p16/Rb and the ability to grow in soft agar medium. Compared with pre-N0005 cells, post-N0005 cells were significantly ($p<0.001$ by the Student t test) more resistant to the killing activity of seven DNA-modifying agents: camptothecin, etoposide, bleomycin, fluorouracil, thioguanine, melphalan and actinomycin D. However, both pre-N0005 and post-N0005 cells showed similar levels of cytotoxicity against four DNA-non-modifying agents: colchicine, paclitaxel, vincristine and methotrexate. DNA-modifying and DNA-non-modifying agents are distinguished by their different sensitivities with pre-N0005 and post-N0005. Based on these results, we propose that pre-N0005 and post-N0005 cell lines be used as a new method to assess and screen anticancer agents.

Key words anticancer agent; assessment; screening; immortalized cell line; DNA-modifying agent

An anticancer drug screening program based on the use of multiple panels of human solid tumor cell lines was developed in the United States,[1] and a similar system using a panel of 60 human tumor cell lines organized into subpanels representing leukemia, melanoma, and cancers of the lung, colon, kidney, ovary, and central nervous system was also developed.[2] Vassilev *et al.*[3] used a cell-based screening approach for anticancer drugs by using sensitivity differences between normal and cancer cells. For these studies, diploid adherent cells—if used, including fibroblasts, are mainly used as a control cell line. A potential problem in these systems is that most control cells do not necessarily have a high proliferating activity, and do not show a high sensitivity to anticancer agents. Anticancer agents have strong side effects in actively proliferating cells, such as haemapoietic cells, lymphoid cells, gut epithelial cells and hair root cells causing anemia, lymphopenia, diarrhea, and loss of hair. Therefore, easily available control cell lines with actively proliferating activity are required.

Human resting B-cells from peripheral blood are easily transformed by Epstein–Barr virus (EBV) to actively proliferating lymphoblastoid cell lines (LCLs). These LCLs with normal diploid karyotypes have long been believed to be "immortal", without becoming tumorigenic.[4—6] A series of recent studies, however, indicate that this initial, simple concept needs extensive reconsideration.[7—11] Most conventionally established LCLs from normal individuals are mortal (pre-immortal) because their telomeres shorten.[12] Some LCLs are truly immortalized (post-immortal) by overcoming the proliferation crisis, accompanied by developing strong telomerase activity and abnormal chromosomes including aneuploidy, after chromosomal rearrangement.[11,13,14] Post-immortal LCLs undergo other changes during long-term culture[15—17]: down-regulation of p16/Rb, mutation of the *p53* gene, modulation of apoptosis and sensitivity to chemical agents. Some post-immortal LCLs develop the ability to form colonies in agarose, and even become tumorigenic by developing the ability to grow in nude mice. Notably, pre-immortal LCL cells share various characteristics with normal B-lymphoblasts generated *in vivo* by antigen stimulation, providing a basis to use pre-immortal LCLs as a control cell line representing actively proliferating normal lymphoblasts.[6,18] Normal lymphoblasts and LCL cells share the following characteristics: lymphoblastoid morphology, surface immunoglobulin, secretion of immunoglobulin, a limited lifespan (mortal), negative or low telomerase activity and normal diploid chromosomes. If pre- and post-immortal LCLs derived from a common cell line show different cytotoxicity against anticancer agents, the difference is considered to be solely due to immortalization. Therefore, we used post-immortal LCLs (post-LCLs) as a model of lymphoma and pre-immortal LCLs (pre-LCLs) as a control.

Anticancer agents are roughly divided into two groups: 1) DNA-modifying agents that modify DNA by nicking DNA to create a strand break (*e.g.*, by camptothecin, etoposide, bleomycin), by alkylating DNA (*e.g.*, by melphalan), by being incorporated into DNA sequence instead of normal DNA precursors (*e.g.*, by fluorouracil,[19] thioguanine[20]) or by inserting into double strand DNA by intercalation (*e.g.*, by actinomycin D); and 2) DNA-non-modifying agents[21] that have anticancer activity by affecting the cytoplasmic constituents, including microtubules (*e.g.*, by colchicine, vincristine, paclitaxel) and by inhibiting the synthesis of DNA precursors (*e.g.*, by methotrexate). Fluorouracil and thiguanine have also the activity to inhibit the synthesis of DNA precursors.[21]

In this study we aimed to show that these DNA-modifying and DNA-non-modifying agents have different modes of action with pre- and post-LCLs. We also suggest that pre- and post-LCLs are used as tools to screen and assess anticancer agents.

MATERIALS AND METHODS

Anticancer Agents The following anticancer agents were obtained from Sigma Chemical Co., Ltd. (St. Louis,

* To whom correspondence should be addressed. e-mail: sugimoto@genecare.co.jp

Table 1. Characteristics of Pre- and Post-LCLs

Items	Pre-N0005 and Pre-N6803	Post-N0005	Post-N6803	Post-N6803-2
Chromosome	Normal diploid (2n)	Abnormal (near 4n)	Abnormal (near 2n)	Abnormal (near 2n)
Telomerase	−/+	+++	+++	+++
p16/pRb	+++	+	−	−/+
p53	Normal	Mutation	Normal	Normal
Colony formation	−	+	+	−
Growth in nude mice	−	−	+	−

This table is based on the data of refs. 13, 14, 16.

Missouri, U.S.A.): melphalan, thioguanine, fluorouracil, methotrexate, actinomycin D, bleomycin, colchicine, vincristine, etoposide, camptothecin, paclitaxel. These agents were dissolved in dimethyloxide (DMSO) before use.

Cell Lines The LCLs were reported previously,[12,13,18] including their characteristics, such as telomerase activity and telomere length. Table 1 compares the characteristics of post-N0005, post-N6803 and post-N6803-2 with their counterparts, pre-N0005 and pre-N6803.[13,14,16] All post-LCLs had high telomerase activity, abnormal chromosomes, and down regulation of p16/pRb. Both post-N0005 and post-N6803 form colonies in soft agarose medium and post-N6803 grow in nude mice.[16] Post-N0005 has a mutation of the *p53* gene. Notably, post-N6803-2, derived from pre-N6803, has neither colony-forming activity in soft agarose medium nor growth activity in nude mice, which are the characteristics of post-N6803.[16]

The method to establish LCLs was reported previously.[12] Briefly, peripheral blood cells were infected with EBV propagated in marmoset cell line B95-8[4] in the presence of 200 ng/ml of ciclosporin (Sandoz, Switzerland). Established LCL cells were cultured in 5 ml RPMI1640 medium (Nissui Pharmaceutical Co., Ltd., Tokyo) supplemented with fetal calf serum (Gibco) in 25 cm^2 bottles (Corning, NY, U.S.A.) that stood on a level surface. The cells were passaged twice a week by exchanging half a cell suspension with fresh medium. A T-cell leukemia cell line, Molt-4, was used as a reference. Fibroblasts TIG-3, derived from human fetal lung, and HeLa cells were cultured with Dulbecco's modified Eagle's medium (Sigma) containing 10% fetal bovine serum (Gibco) containing gentamycin. All cell lines, except pre- and post-N0005, were used as references of N0005.

Cytotoxicity Assay Cultured cells were harvested two days after a medium change, and 100 μl of cell suspension were seeded to each well of a 96-well culture plate on day 0. The number of cells in each well was: 50000 pre-N0005; 25000 post-N0005; 5000 TIG; 1500 HeLa. On day 1, an anticancer agent in 10 μl DMSO was added to each well and 10 μl DMSO without the agent was added to control wells. On day 3, the number of viable cells was assessed by using WST-8 (2-(2-methoxy-4-nitrophenyl)-3-(4-nitrophenyl)-5-(2,4-disufophenyl)-2*H*-tetrazolium, monosodium salt) by using the kit protocol (Nacalai Tesque Co., Ltd., Kyoto). Briefly, 10 μl of WST-8 solution was added to each well, and then the plates were incubated at 37 °C for 3—4 h in a 7.5% CO_2 incubator atmosphere. The absorbance was measured by using a Multilabel counter ARVO HTS (Perkin Elmer) at a test wavelength of 450 nm with a reference wavelength of 620 nm. To determine the IC_{50}, the final concentration of the anticancer test agent was serially diluted usually by 1/2 by medium and a similar dilution of DMSO without the agent was used for the controls without the agent. Each assay, as well as the whole experiment, was done at least three times, giving more than nine values of IC_{50}.

Analysis by Flow Cytometry The cells were fixed with 70% ethanol at 4 °C for 1 h. A 25 μl aliquot of 10 mg/ml RNase (Sigma) solution was added to a 1 ml cell suspension (1×10^6/ml) in phosphatebuffered saline, and the mixture was incubated at 37 °C for 30 min. Propidium iodide (Sigma) solution (0.1 ml at 500 μg/ml) was added to the cell suspension, and then the mixture stood at 4 °C for 30 min in the dark. The cell cycle distribution was analyzed by using a Coulter Epics XL flow cytometer (Beckman Coulter Co., Ltd, Tokyo).

Statistical Analysis A Student *t* test was done for the values of IC_{50} of two different groups, including between pre- and post-N0005, between pre-N0005 and Molt-4, between pre- and post-N6803 and between TIG-3 and HeLa.

RESULTS

Analysis by Flow Cytometry Figures 1A and B show profiles of the flow cytometry analysis of pre- and post-N0005 treated with or without various anticancer agents. Pre-N0005 cells are diploid (2n), but post-N0005 cells are near tetraploid (4n). Both colchicine and paclitaxel induced accumulation of G2/M cells. In cells treated with camptothecin and actinomycin D, G1/S was stopped with the apparent disappearance of a G2/M peak. The mode of action of anticancer agents was similar in pre- and post-N0005 cell lines as judged by the profiles of flow cytometry.

Cytotoxic Effects of Anticancer Agents on Pre-N0005 and Post-N0005 Figures 2A and B show the effect of 11 anticancer agents on pre- and post-N0005. Three G2/M inhibitors (colchicine, vincristine and paclitaxel) and one G1/S inhibitor (methotrexate) showed similar levels of cytotoxicity in pre- and post-N0005 (Fig. 2A). Tables 2 and 3 summarize the values of Fig. 2; the tables show, for convenience, the IC_{50} ratio (pre-/post-). An IC_{50} ratio less than 1 means that an agent shows stronger cytotoxicity in pre- than post-N0005 cells, and an IC_{50} ratio of about 1 means that an agent has a toxicity similar in pre- and post-N0005. However, seven G1/S inhibitors (fluorouracil, thioguanine, melphalan, bleomycin, actinomycin D, camptothecin and etoposide) showed markedly stronger cytotoxicity in pre- than post-N0005 (Fig. 2B). The difference in pre- and post-N0005 was statistically significant ($p<0.001$) (Table 2). Especially marked was the difference in the effect of bleomycin in pre- and post-N0005 cells. Methotrexate and the three G2/M inhibitors do not, but the remaining seven G1/S inhibitors do, directly modify DNA strands. Thus, for these 11 anticancer

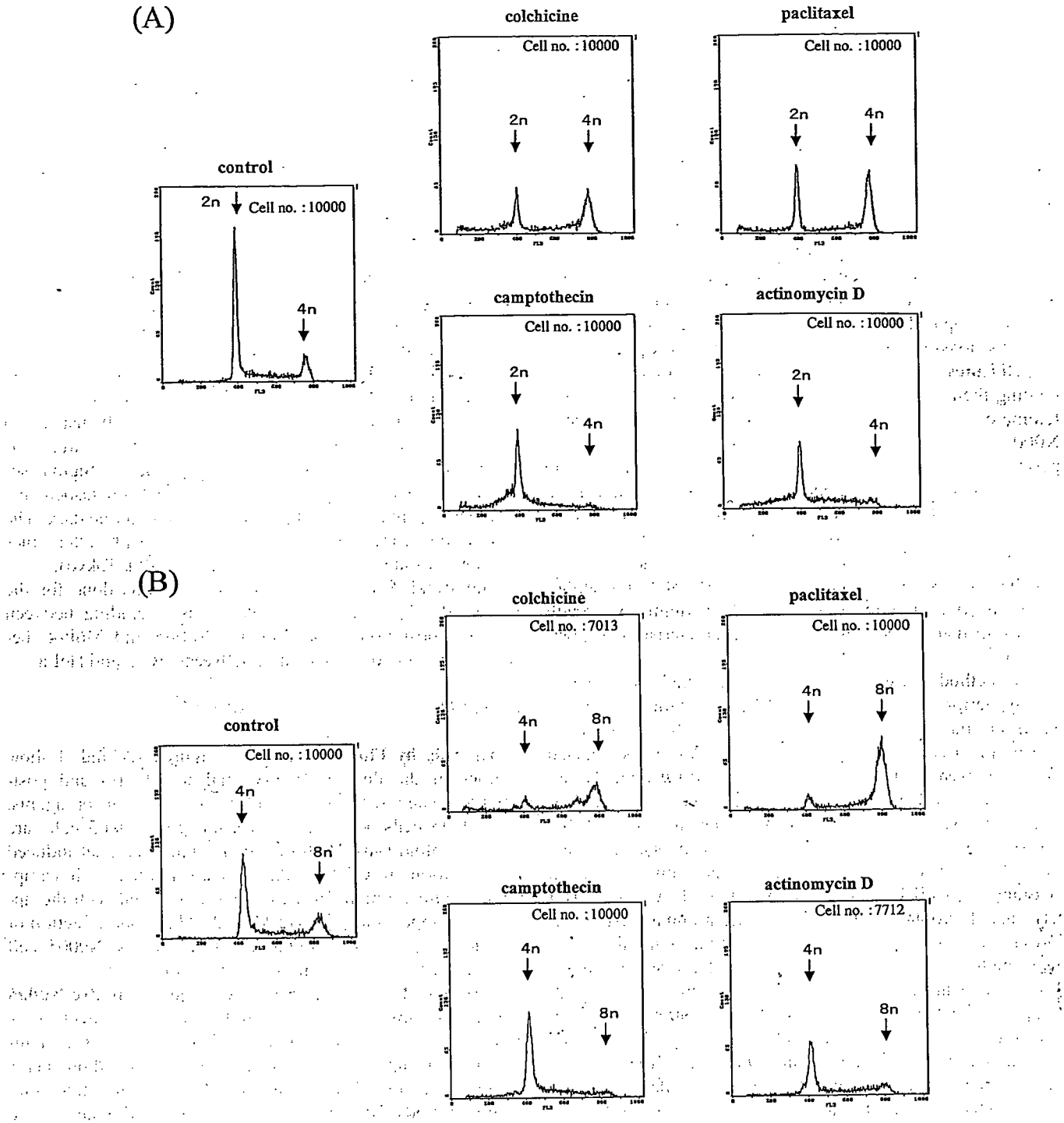

Fig. 1. Flow Cytometric Analysis of Pre-N0005 (A) and Post-N0005 (B) Cells Treated with 4 μM of Anticancer Agents for 12 h
"Control" indicates cells without treatment.

agents, all DNA-modifying agents showed stronger cytotoxicity in pre- than post-N0005 (IC_{50} ratio of less than one), but all DNA-non-modifying agents showed similar cytotoxicity in both pre-N0005 and post-N0005 (IC_{50} ratio of nearly 1). Figure 1C and Table 3 show the effect of colchicine and camptothecin in pre- and post-N6803 cells. Colchicine showed similar levels of cytotoxicity in pre- and post-N6803, but etoposide showed stronger cytotoxicity in pre- than in post-N6803. These results of using colchicine and etoposide, together with our preliminary results (data not shown) of using vincristine, paclitaxel, methotrexate, bleomycin and camptothecin, showed a similar tendency as for pre- an post-N0005. That is, DNA-non-modifying agents showe similar levels of cytotoxicity in pre- and post-N6803, bu DNA-modifying agents showed stronger cytotoxicity in pre than post-N6803. Table 2 shows also the IC_{50} of each ager as a reference in Molt-4 that is a post-immortal T-ce leukemic line. The result obtained for pre- and post-N000 was not obtained for pre-N0005 and Molt-4. For exampl bleomycin that had almost no cytotoxicity in post-N000 showed similar levels of cytotoxicity in pre-N0005 and Mol 4.

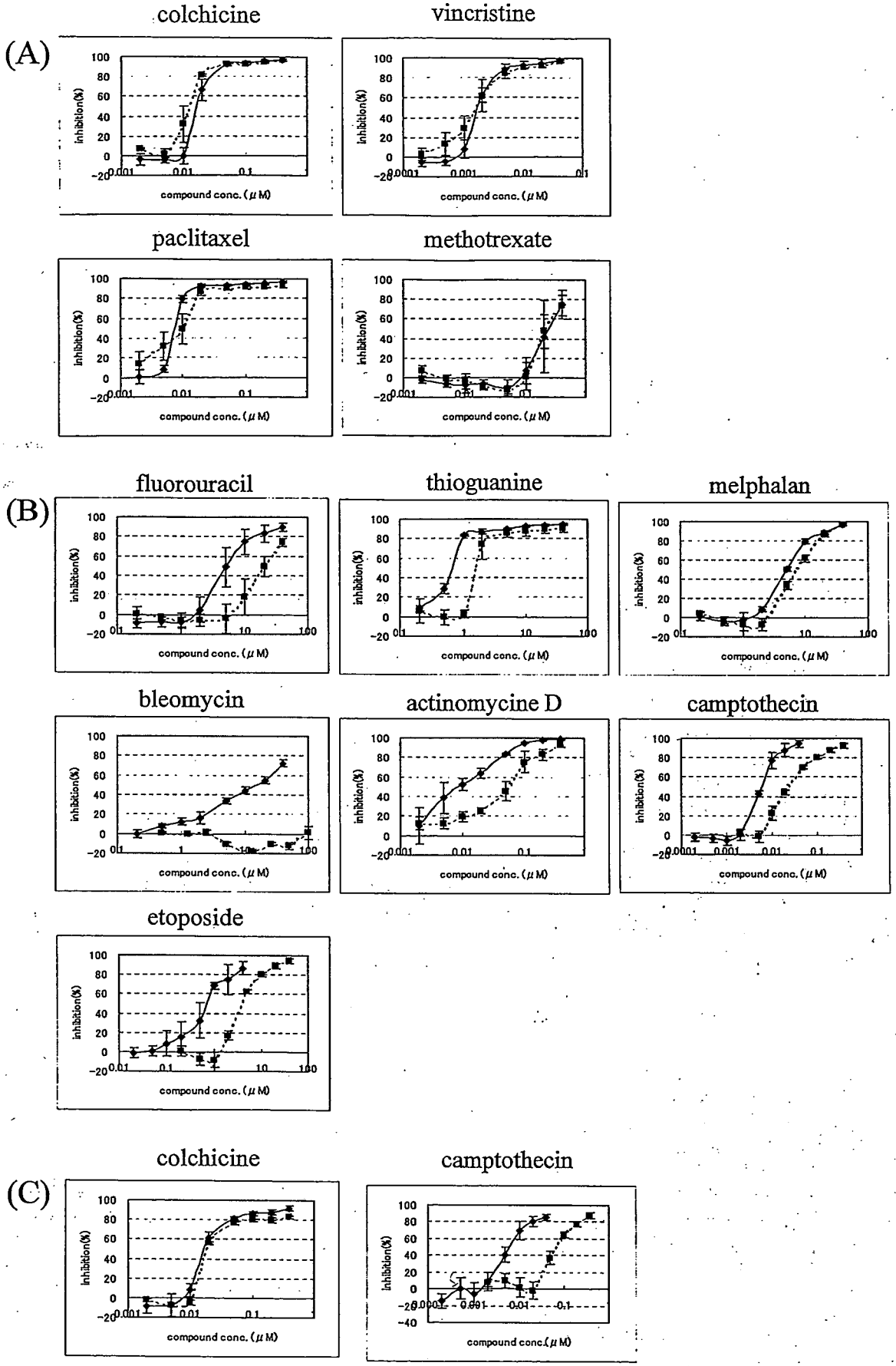

Fig. 2. Effects of Four DNA-Non-modifying Agents (A) and Seven DNA-Modifying Agents (B) on Pre-N0005 (Solid Line) and Post-N0005 (Dotted Line) Cells and Effects of Colchicine and Camptothecin on Pre-N6803 (Solid Line) and Post-N6803 (Dotted Line) Cells (C)

The vertical axis indicates inhibition (%) of cell growth and the horizontal line indicates the final concentration of agent added to the medium (μM).

Table 2. Cytotoxic Effects of Anticancer Agents on Pre-N0005, Post-N0005 and Molt-4 Cells

Anticancer agents	Inhibition in cell cycle	DNA modification	N0005 (pre)		N0005 (post)		Pre/post[c]	Molt-4		Pre/Molt-4[d]
			IC_{50}[a]	S.D.[b]	IC_{50}	S.D.		IC_{50}	S.D.	
Colchicine	G2/M	No	0.019	0.002	0.016	0.003	1.1*	0.026	0.00	0.7**
Vincristine	G2/M	No	0.0018	0.0002	0.0017	0.0003	1.0*	0.0029	0.00	0.6**
Paclitaxel	G2/M	No	0.0080	0.0005	0.0091	0.0022	0/9*	0.0077	0.0007	1.0*
Methotrexate	G1/S	No	0.18	0.01	0.19	0.02	1.0*	0.05	0.00	3.9**
Fluorouracil	G1/S	Yes	4.5	0.8	23	4	0.2**	13.3	2.1	0/3**
Thioguanine	G1/S	Yes	0.6	0.0	1.92	0.24	0.3**	1.32	0.19	0.5**
Melphalan	G1/S	Yes	5.3	0.1	7.7	0.45	0.7**	4.55	0.76	1.2*
Bleomycin	G1/S	Yes	13.4	0.7	>100	—	<0.2**	13.42	1.3	1.0*
Actinomycin D	G1/S	Yes	0.011	0.001	0.049	0.012	0.2**	0.02	0.00	0.5**
Camptothecin	G1/S	Yes	0.0057	0.0002	0.028	0.00	0.2**	0.0086	0.00	0.7**
Etoposide	G1/S	Yes	0.6	0.1	4.4	0.24	0.1**	0.28	0.05	2.0**

a) μM, *b*) standard deviation, *c*) ratio of pre-N0005 and post-N0005 in IC_{50}, *d*) ratio of pre-N0005 and Molt-4 in IC_{50}. —: data not available, * statisitically not significant, ** statistically significant ($p<0.001$) between pre- and post-N0005 or between pre-N0005 and Molt-4.

Table 3. Cytotoxic Effects of Anticancer Agents on Pre-N6803 and Post-N6803 Cells

Anticancer agents	Inhibition in cell cycle	DNA modification	N6803 (pre)		N6803 (post)		Pre/post[c]
			IC_{50}[a]	S.D.[b]	IC_{50}	S.D.	
Colchicine	G2/M	No	0.020	0.00	0.021	0.00	1.0*
Camptothecin	G1/S	Yes	0.0076	0.00	0.076	0.01	0.1**

a) μM, *b*) standard deviation, *c*) ratio of pre-N6803 and post-N6803 in IC_{50}. * Statistically not significant, ** statistically significant ($p<0.001$) between pre-N6803 and post-N6803.

Table 4. Cytotoxic Effects of Anticancer Agents on TIG3 and HeLa Cells

Anticancer agents	Inhibition in cell cycle	DNA modification	TIG-3		HeLa		TIG-3/HeLa[c]
			IC_{50}[a]	S.D.[b]	IC_{50}	S.D.	
Colchicine	G2/M	No	0.02	0.00	0.020	0.00	0.9*
Vincristine	G2/M	No	0.01	0.00	0.002	0.000	2.6**
Paclitaxel	G2/M	No	0.01	0.00	0.002	0.000	6.8**
Methotrexate	G1/S	No	>100	—	>100	—	—
Fluorouracil	G1/S	Yes	34	3.5	>40	—	<0.8*
Thioguanine	G1/S	Yes	18.4	2.2	6.6	1.2	2.8**
Melphalan	G1/S	Yes	27.35	5.26	70.9	12.2	0.4*
Bleomycin	G1/S	Yes	12.70	3.21	>40	—	<0.32**
Actinomycin D	G1/S	Yes	0.016	0.003	0.0086	0.0014	1.8**
Etoposide	G1/S	Yes	18.83	1.67	>40	—	<0.5**
Camptothecin	G1/S	Yes	0.98	0.34	1.20	0.30	0.8*

a) μM, *b*) standard deviation, *c*) proportions of TIG-3 and HeLa in IC_{50}. —: data not available. * Statisitically not significant, ** statistically significant ($p<0.001$) between TIG-3 and HeLa.

Cytotoxic Effects of Anticancer Agents in TIG-3 and HeLa Cells Table 4 summarizes the cytotoxic effects of the 11 anticancer agents in TIG-3 and HeLa cells. The mode of effect of anticancer agents in these cell lines is different from that in pre- and post-N0005 cells. Methotrexate and fluorouracil showed weak effects in TIG-3 and HeLa cells. The effect of DNA-modifying and non-modifying agents in TIG-3 and HeLa cells showed no apparent constant difference.

DISCUSSION

In this study, 4 of 11 anticancer agents without DNA-modifying activity showed similar levels of cytotoxicity in both pre- and post-N0005 cells, but all remaining 7 agents with DNA-modifying activity showed less cytotoxicity in post- than pre-N0005 cells. Because pre- and post-N0005 cells have the same cellular background—even though post-N0005 is immortalized with up-regulation of telomerase, abnormal chromosomes, down regulation of p16/Rb, mutation of *p53* gene, and has the ability to grow in soft agarose medium—the increased resistance to DNA-modifying agents is probably linked with factors related to immortalization. In N0005 cells, the expression level of WRN helicase, the product of the causative gene of Werner syndrome, is up-regulated after immortalization.[16,22] WS patient LCLs and mouse embryonic stem cells lacking normal WRN helicase are more sensitive to camptothecin than corresponding cells with normal WRN helicase,[15,23] which at least partly explains why post-N0005 cells are more resistant to camptothecin than pre-N0005 cells. Similarly, up-regulation of gene products in DNA repair could be responsible for the increased resistance of post-N0005 cells to DNA-modifying agents.

Post-N6803 cells showed resistance to DNA-modifying agents, but post-N6803-2, derived from the original cell line (pre-N6803) as post-N6803, showed less resistance to DNA-modifying agents: post-N6803-2 showed high sensitivity to camptothecin (IC_{50} 0.0074 μM), etoposide (IC_{50} 0.12 μM), fluorouracil (IC_{50} 1.10 μM) and bleomycin (IC_{50} 0.40 μM) (unpublished preliminary data). Thus, immortalization does not necessarily cause resistance to DNA-modifying agents. Because both post-N0005 and post-N6803, but not post-N6803-2, can form colonies on soft agarose medium,[16] the colony-forming ability might be related to the resistance to DNA-modifying agents. The IC_{50} ratio for pre-N0005 and Molt-4 varied from 0.3 to 2.0 depending on the DNA-modifying agent. These results together imply that linkage between immortalization and increased resistance to DNA-modifying agents is not necessarily general.

The results of this study suggest that pre- and post-N0005 cell lines can be used to assess and screen anticancer agents. Agents against pre-N0005 and post-N0005 that have an IC_{50} ratio less than 1 are possibly DNA-modifying agents, and agents against these cell lines that have an IC_{50} ratio near 1 are possibly DNA-non-modifying agents. In this study, pre-N0005 and post-N0005 had an IC_{50} ratio of either 1 or less, not markedly exceeding 1, with all the 11 anticancer agents, meaning that the cytotoxicity of these agents in pre-N0005 was equal to or stronger than post-N0005, and anticancer agents are few, if any, that show markedly stronger cytotoxicity in post-N0005 than in pre-N0005. These results, together with the fact that pre-N0005 cells are similar to lymphoblastoid cells generated by antigen stimulation, suggest that most anticancer agents available now have the defect that they have strong adverse effects on actively proliferating normal cells. An agent that induces a markedly higher IC_{50} ratio value in pre-N0005 than in post-N0005, meaning that the agent has a markedly stronger cytotoxicity in post- than in pre-N0005 cells, could be an ideal anticancer drug to overcome such a defect, because such an agent is expected to have weaker side effects in actively proliferating hematopoietic cells, lymphoblasts, hair-root cells and gut epithelial cells.

Recently, we observed that the expression of many genes is up- and down-regulated accompanied by immortalization, including the gene of human telomerase reverse transcriptase, as shown by using a micro-array of DNA chip (unpublished observation). The correlation of this phenomenon with the resistance of post-LCLs against anticancer agents is an interesting problem to be elucidated.

Lastly, we like also note that pre-LCL cells and normal B-lymphoblasts are apparently different to each other in the following points although they share many properties as discussed thus far. Pre-LCLs have usually a very long lifespan which is probably much longer than the lifespan of normal B-lymphoblasts.[11,14] Lymhoproliferative disease caused by increase of EBV-transformed lymphoblastoid cells, probably mostly corresponding to pre-LCL cells, by reactivation of EBV after bone-marrow transplantation is known to respond poorly to standard therapy although they could be cured by the infusion with EBV-specific donor-type T-cell lines.[24] Thus, these facts should be taken into consideration when pre-LCL cells are used as a control in assessment and screening of anticancer agents.

To conclude, post-N0005 cells could be used as models of lymphoma cells and pre-N0005 as control cells to assess and screen anticancer agents.

REFERENCES

1) Alley M. C., Scudiero D. A., Monks A., Hursey M. L., Czerwinski M. J., Fine D. L., Abbott B. J., Mayo J. G., Shoemaker R. H., Boyd M. R., *Cancer Res.*, **48**, 589—601 (1988).
2) Monks A., Scudiero D., Skehan P., Shoemaker R., Paull K., Vistica D., Hose C., Langley J., Cronise P., Vaigro-Wolff A., Gray-Goodrich M., Cambell H., Nayo J., Boyd M., *J. Natl. Cancer Inst.*, **83**, 757—766 (1991).
3) Vassilev L. T., Kazmer S., Marks I. M., Pezzoni G., Sala F., Mischke S. G., Foley L., Berthel S. J., *Anticancer Drug Des.*, **16**, 7—17 (2001).
4) Miller G., Fields B. N., Knipe K. M. (eds.), "Virology," Raven Press, New York, 1990, pp. 1921—1958.
5) Nilsson K., "The Nature of Lymphoid Cell Lines and Their Relationship to the Virus," Springer-Verlag, New York, 1979.
6) Nilsson K., *Hum. Cell*, **5**, 25—41 (1992).
7) Counter C. M., Avilion A. A., LeFeuvre C. E., Stewart N. G., Greider C. W., Harley D. B., Bacchetti S., *EMBO J.*, **11**, 1921—1929 (1992).
8) Counter C. M., Botelho F. M., Wang P., Harley C. B., Bacchetti S., *J. Virol.*, **68**, 3410—3414 (1994).
9) Sugimoto M., Ide T., Goto M., Furuichi Y., *Mech. Ageing Dev.*, **107**, 51—60 (1999).
10) Sugimoto M., Ide T., Goto M., Furuichi Y., *J. Virology*, **73**, 9690—9691 (1999).
11) Sugimoto M., Tahara H., Ide T., Furuichi Y., *Cancer Res.*, **64**, 3361—3364 (2004).
12) Tahara H., Tokutake Y., Maeda S., Kataoka H., Watanabe T., Satoh M., Matsumoto T., Sugawara M., Ide T., Goto M., Furuichi Y., Sugimoto M., *Oncogene*, **15**, 1911—1920 (1997).
13) Okubo M., Tsurukubo Y., Higaki T., Kawabe T., Goto M., Murase T., Ide T., Furuichi Y., Sugimoto M., *Cancer Genet. Cytogenet.*, **129**, 30—34 (2001).
14) Sugimoto M., Tahara H., Okubo M., Kobayashi T., Goto M., Ide T., Furuichi Y., *Cancer Genet. Cytogenet.*, **152**, 95—100 (2004).
15) Okada M., Goto M., Furuichi Y., Sugimoto M., *Biol. Pharm. Bull.*, **21**, 235—239 (1998).
16) Takahashi T., Kawabe T., Okazaki Y., Itoh C., Noda K., Tajima M., Satoh M., Goto M., Mitsui Y., Tahara H., Ide T., Furuichi Y., Sugimoto M., *DNA Cell Biol.*, **22**, 727—735 (2003).
17) Satoh M., Yasuda T., Higaki T., Goto M., Tanuma S., Ide T., Furuichi Y., Sugimoto M., *Cell Struct. Funct.*, **28**, 61—70 (2003).
18) Kataoka H., Tahara H., Watanabe T., Sugawara M., Ide T., Goto M., Furuichi Y., Sugimoto M., *Differentiation*, **62**, 203—211 (1997).
19) Lonn U., Lonn S., Nylen U., Winblad G., *Cancer Res.*, **49**, 1085—1089 (1989).
20) Warren D. J., Slordal L., *Anal. Biochem.*, **215**, 278—283 (1993).
21) Skeel R. T., "Handbook of Cancer Chemotherapy," Fifth ed., Lippincott Williams & Wilkins, New York, 1999.
22) Shiratori M., Sakamoto S., Suzuki N., Tokutake Y., Kawabe Y., Enomoto T., Sugimoto M., Goto M., Matsumoto T., Furuichi Y., *J. Cell Biol.*, **144**, 1—9 (1999).
23) Lebel M., Leder P., *Proc. Natl. Acad. Sci. U.S.A.*, **95**, 13097—13102 (1998).
24) Rooney C. M., Smith C. A., Ng C. Y., Loftin S., Li C., Krance R. A., Brenner M. K., Heslop H. E., *Lancet*, **345**, 9—13 (1995).

Quantitative Analysis of Werner Helicase Activity Using the Single-Molecule Fluorescence Detection System MF10S

Kazunobu FUTAMI, Hideyuki GOTO, Akira SHIMAMOTO, Takahide WATANABE, and Yasuhiro FURUICHI*

GeneCare (previously AGENE) Research Institute; 200 Kajiwara, Kamakura, Kanagawa 247–0063, Japan.
Received August 9, 2004; accepted September 19, 2004

We developed a system that uses the single-molecule fluorescence detection system MF10S to assess quantitatively the activity of WRN helicase, the product of the causative gene of Werner syndrome that includes premature ageing. Double-strand DNA substrates labeled with the fluorescence dye TAMRA at the 5′ end and with a quencher at the 3′ end of the counter strand were incubated with a single trapper oligonucleotide and Werner helicase, and the resultant single DNA fragments labeled with TAMRA produced by the unwinding of WRN helicase were detected using the MF10S. The results using this system and those using polyacrylamide gel electrophoresis were well correlated. The MF10S system provides a quantitative analysis that is much faster, simpler, and more economical than systems using polyacrylamide gel electrophoresis and radioisotopes, and could be used as a quantitative analysis system for Werner helicase and other DNA helicase activities.

Key words helicase assay; screening system; anti-cancer drug

Inhibitors of DNA helicases have potential applications to screen anti-virus and anti-tumor drugs. The screening of compounds to inhibit helicases of hepatitis C virus (NS3), herpes simplex virus (UL5), and papillomavirus has been reported.[1—4] WRN helicase, the product of the causative gene of Werner syndrome, unwinds double-strand DNA.[5,6] Short interference RNAs (siRNAs) with WRN gene sequences inhibit the expression of WRN helicase in HeLa cells resulting in genomic instability (Futami *et al.*, unpublished results). Cells lacking WRN helicase have increased sensitivity to cytotoxicity by camptothecin.[7] Thus, the development of a system to quantitatively assay DNA helicases, including WRN helicase, is necessary not only for research, but also for highly sensitive screening of anti-virus and anti-cancer drugs without using radioisotopes. We report here a system enabling the DNA-unwinding activity of Werner helicase to be quantitatively assayed and monitored using the single-molecule fluorescence detection system MF10S.

MATERIALS AND METHODS

Sequences of the double-strand DNA substrate were: 1) donor strand oligonucleotide, 5′-TAMRA (6-carboxytetramethylrhodamine)-TAGTACCGCCACCCTCAGAACCTTTTTTTTTTTTTTT; and 2) acceptor strand, 5′-TAGTACCGCCACCCTCAGAACC-BHQ (Black Hole Quencher)-2; 3) A-trapper, 5′-TAGTACCGCCACCCTCAGAACC; 4) B-trapper, 5′-GGTTCTGAGG-GTGGCGGTACTA. Actinomycin D, adenosine 5′-*O*-(3-thiotriphosphate) (ATP-γ-S) and SYBR Gold (SYBR® Gold) were purchased from Sigma (St. Louis), Roche Diagnostic (Tokyo) and Molecular Probes (Oregon), respectively. TAMRA- and BHQ-2-labeled oligonucleotides were obtained from Hokkaido System Science Co., Ltd. (Sapporo). The substrate oligonucleotide DNAs were prepared by heating single oligonucleotides at 90 °C for 5 min and then by cooling to room temperature. TAMRA is a stable dye, and BHQ-2 is a highly efficient quencher that strongly prevents fluorescence of TAMRA without emitting its own fluorescence leading to a low background. This TAMRA/BHQ-2 system has an advantage over a system using a quencher that is based on a distance-dependent fluorescence resonance energy transfer.[8—10]

Preparation of WRN Helicase WRN helicase was expressed using the baculovirus vector/Sf9 system, and was purified as previously reported.[11] Briefly, infected cells were collected and resuspended in ice-cold PBS and the recombinant proteins were purified by 6×His affinity chromatography.

Helicase Assay The reaction conditions for WRN helicase activity were optimized with 50 μl of reaction mixture containing 50 mM Tris–HCl (pH 7.5), 2 mM 2-Mercapto ethanol, 5 mM $MgCl_2$, 1 mM ATP, 20 μg/ml bovine serum albumin, 90 mM NaCl, 5 nM WRN helicase, 2 nM DNA substrate, and the trapper single strand DNA at various concentrations in glass bottom 96-well plates (Whatman, Clifton, NJ, U.S.A.). The reaction was done at 37 °C for the indicated period shown as the "reaction time" in each figure, and then was stopped by adding 10 μl of 5× stopping dye solution containing 0.1% xylene cyanol (Nacalai Tesque, Kyoto), 100 mM Tris–HCl, and 50% glycerol. The reaction mixtures in 96-well plates were read using an Olympus MF10S (543 nm, laser power; 300 μW, 0.5 S) three times for each well, and an aliquot of each reaction mixture was analyzed using 15% polyacrylamide gel electrophoresis (PAGE) with an electrophoresis buffer (pH 8.5) consisting of 0.09 M Tris–borate and 2 mM ethylenediaminetetraacetic acid (EDTA). After electrophoresis (20 min, 200 V/4 cm), the gel was visualized by laser scanning in an fluorescent image analyzer FMBIO® II Multi-View and FMBIO Analysis version 6.0 software (Hitachi Software Engineering, Yokohama).

Fluorescence Detection System MF10S We used a MF10S (Olympus) single-molecule fluorescence detection system for quantitative analysis of unwound TAMRA-labeled DNA strands. This system permits the detection of fluorescent signals coming from a small volume (10^{-15} l) of reaction mixture by the optics of a confocal microscope. Samples at several nanomolar concentrations contain a few molecules in the volume, so signals directly reflect the intensity and the number of fluorescent molecules. The number of fluorescent signals was expressed by the "countrate" that indicates the

* To whom correspondence should be addressed. e-mail: furuichi@genecare.co.jp

number of photons in each second detected in an area being measured.[12]

RESULTS AND DISCUSSION

We chose TAMRA as a reporter because it is easy to label the substrate oligonucleotides and is not expensive. We then compared the sensitivity to detect TAMRA-labeled DNAs between two detection systems, the MF10S and a Wallac multilabel counter (Perkin-Elmer, Tokyo) which is often used for high-throughput screening (HTS) (Fig. 1). The sensitivity with the MF10S system was found to be about 100-fold higher than that of the Wallac system, and moreover, the background associated with MF10S was low, giving rise to the reproducible results. As a result, the combination of TAMRA and MF10S could reduce the amounts of both substrate and enzyme, rendering the system almost equivalent to the radioisotopic system. Based on these results, we applied the MF10S system for helicase assay. An assay system for WRN helicase that uses the MF10S single-molecule fluorescence detection system was assessed under various reaction conditions and the results were compared with the results obtained from PAGE analysis simultaneously done using the same reaction products.

Effect of Trappers WRN helicase unwinds double strand DNA.[6,11,13] The unwinding reaction of double-strand DNA by WRN helicase requires trappers *in vitro* to stabilize the resultant single strand DNA by preventing reannealing.[14] Figure 2 shows the outline of the reaction. The efficiency of two types of trapper oligonucleotides, A-trapper and B-trapper, for binding the unwound DNA strand was compared (Fig. 2A). A-trapper and B-trapper form duplexes with BHQ-2 labeled and TAMRA-labeled strands, respectively. The partially double-stranded DNA substrates consisting of TAMRA-labeled and BHQ-2-labeled strands were mixed with either A-trapper or B-trapper, and the mixture was incubated with Werner helicase. The trappers inhibited re-formation of the duplex between the original substrate DNA strands, making the detection of reaction products more efficient. The fluorescence of TAMRA near BHQ in duplex oligonucleotides was suppressed to very low levels, but the fluorescence of TAMRA in a single oligonucleotide apart from BHQ was strong. Figure 2B shows the results of the analysis using the Olympus MF10S. A-trapper was more efficient than B-trapper, which was confirmed by the assay that used PAGE (Fig. 2C). Therefore, we used A-trapper in the following experiments.

Dose Dependency of A-Trapper Figure 3A shows the dose-dependency of A-trapper in the assay using the MF10S. The unwinding reaction nearly reached a plateau at 50 nM of A-trapper. A similar result was obtained by the independent assay system using PAGE. The good correlation between the results by MF10S and PAGE guarantees that the system using MF10S could be used for quantitative assay of WRN

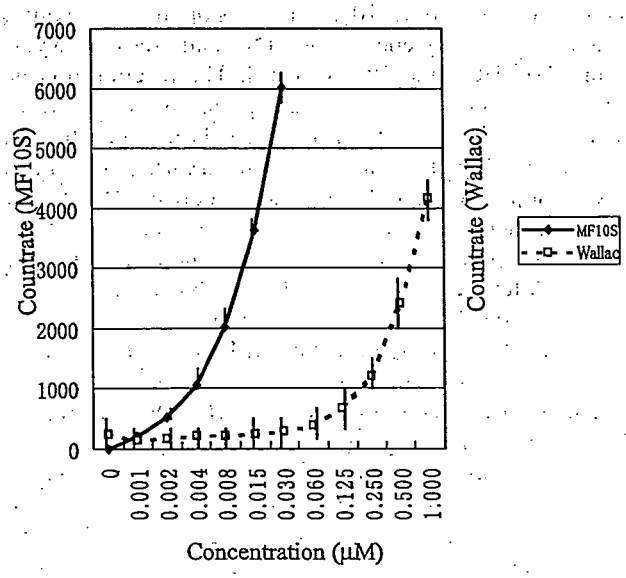

Fig. 1. Comparison of Sensitivity between MF10S and Wallac Systems

The countrate of TAMRA-labeled oligonucleotide was determined either by the MF10S or Wallac system. Vertical and horizontal axes indicate countrate and concentration (μM) of TAMRA-labeled oligonucleotide, respectively. Each point represents a mean of 5 samples and vertical bars indicate standard deviation.

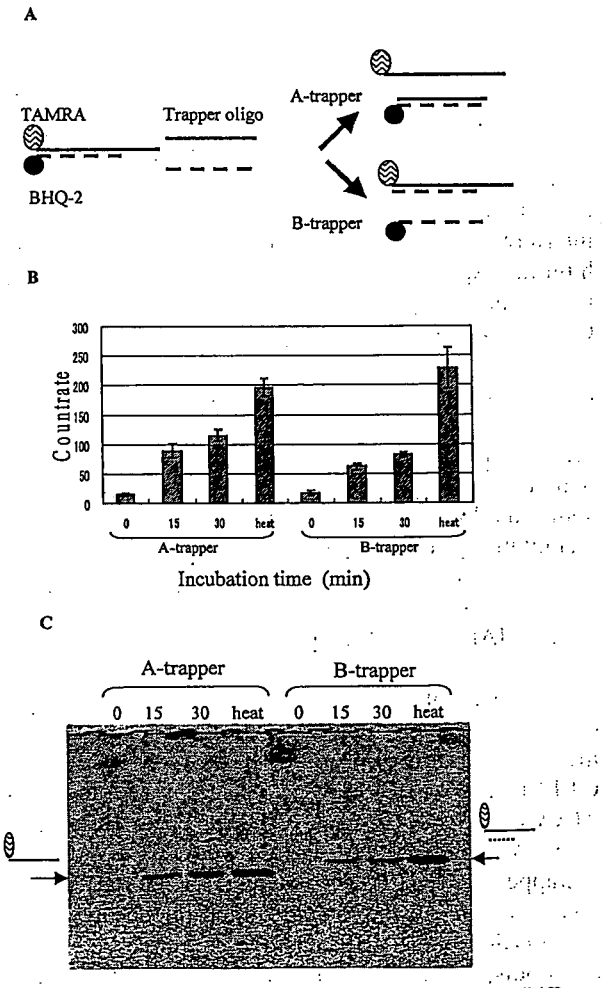

Fig. 2. Assay of Werner Helicase Activity by Using Two Different Oligonucleotides as Trapper Molecules; One Is Complementary to TAMRA-Labeled Oligonucleotide and the Other Is Complementary to BHQ-2-Labeled Oligonucleotide

(A) Two kinds of reaction products forming a duplex with A-trapper or B-trapper are shown. (B) Fluorescence values and the countrate are shown in a Werner helicase reaction with A-trapper or B-trapper by measuring with the MF10S. Each column indicates the mean of three measurements and vertical bars indicate standard deviation. (C) TAMRA fluorescence image in polyacrylamide gel is shown for the same samples of the reaction of B. A TAMRA fluorescence image obtained using an FMBIO II image analyzer. Excitation was 532 nm laser light. The arrows show the position of the TAMRA- labeled oligonucleotide forming a duplex with A-trapper or B-trapper.

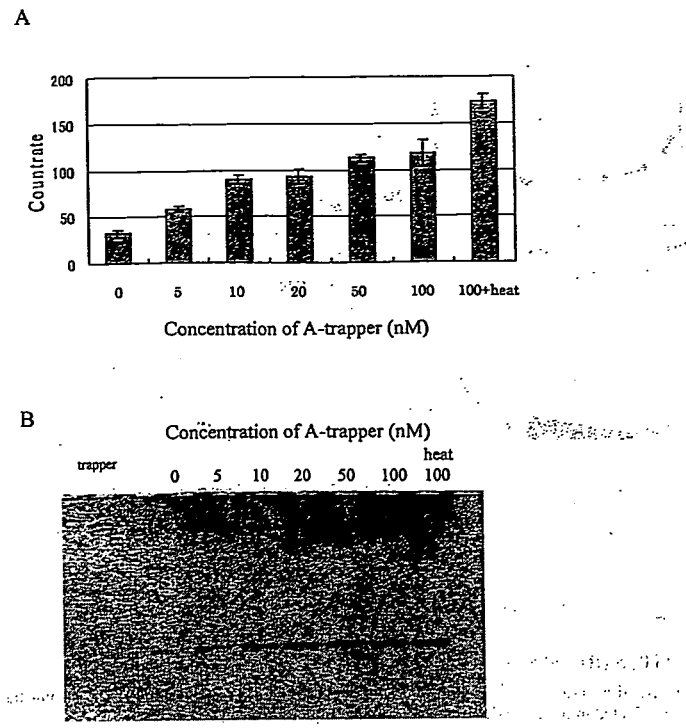

Fig. 3. Dose-Dependency of A-Trapper in a Werner Helicase Reaction, Which Has the Complementary Oligonucleotide Sequence to the BHQ-2-Labeled Sequence

(A) The reaction products are expressed as the countrate using the MF10S. See also the legend of Fig. 2B. (B) The same reaction products are represented as the fluorescence image of TAMRA after the PAGE of each sample.

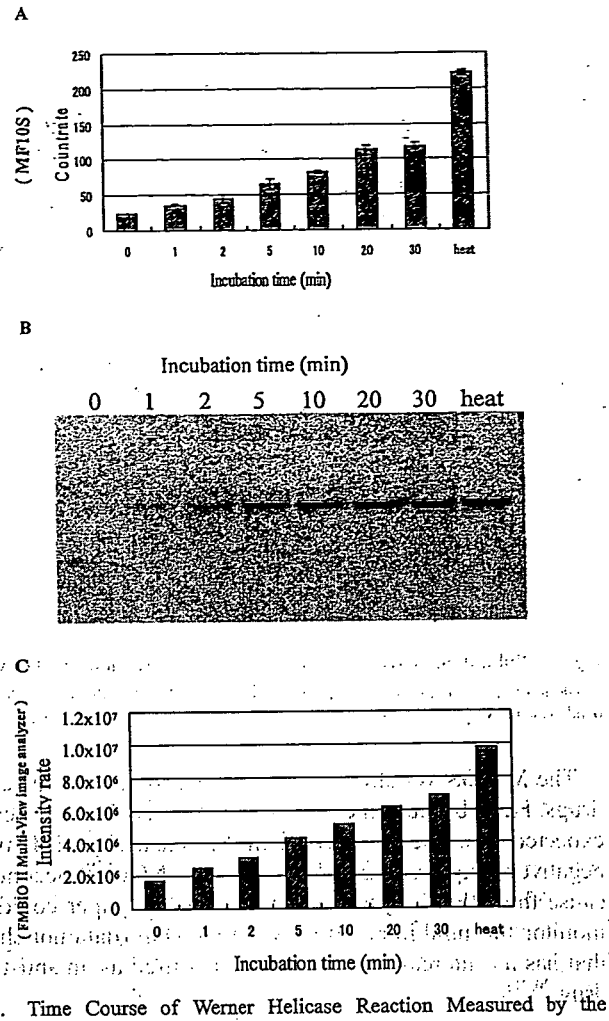

Fig. 4. Time Course of Werner Helicase Reaction Measured by the MF10S (A) and PAGE (B)

See also the legend of Fig. 2B (C). The intensity of fluorescence image of each band was calculated using Image Analysis Software (Hitachi Software Co., Ltd.).

helicase and other DNA helicases instead of PAGE using radioisotopes. The exonuclease consisting of an integral part of Werner helicase[6,15] does not seem to affect the assay system under the conditions tested in this study.

Time Course Figure 4A and 4B show the time course of the reaction using the Olympus MF10S and PAGE, respectively. Figure 4C shows the quantitative intensity of the fluorescence image after the PAGE, which was calculated by image-analysis software. In both assay systems, the reaction nearly reached a plateau after 20 min. Thus, this system can monitor in real-time a helicase-catalyzed reaction process by using the increase in fluorescence.

Effects of Inhibitors The effects of three kinds of inhibitors on Werner helicase activity were investigated to test if the MF10S system can detect inhibitors of WRN helicase. Actinomycin D, an antineoplastic antibiotic that forms a stable complex with DNA, inhibited the activity of Werner helicase at 10 μg/ml (8 μM) or below, reaching a plateau at 20 μg/ml (16 μM) or more, and had a maximal inhibitory effect of about 30% (Fig. 5A, D). ATPγS, which inhibits ATP-dependent enzymes by competing with ATP, showed a more than 60% inhibitory effect at 20 μg/ml (36.6 μM) (Fig. 5B, E). SYBR Gold, a reagent that has a high affinity for DNA and RNA, showed about 70% inhibition at a concentration of 10^{-3} dilution of the original solution when analyzed by a standard 300 nm UV transilluminator. SYBR Gold has strong fluorescence by itself, and it interfered with the assay system (Fig. 5C): The fluorescence of SYBER Gold was visible as strong bands at the top of the PAGE gel (Fig. 5F). These results indicate that the MF10S system can be used as a screening system for compounds that show anti-WRN helicase activity.

Thus far helicase activity has been identified by the reaction products of radioisotope-labeled substrates using PAGE. High-throughput screening systems based on fluorescence resonance energy transfer (FRET) also have been developed.[8,9,16–18] The FRET system is proven to be useful to monitor the reactions catalyzed by helicase, because the results by two systems using radioisotopes and fluorescence coincided very well.[15] Comparing these systems, the MF10S system has the following advantages: 1) the cost of the assay system is cheaper and a high signal-to-noise ratio was achieved by using the strong, dark quencher BHQ. 2) simultaneous monitoring of enzymatic analysis using the same reaction products by MF10S and PAGE is possible, enabling the compounds to be assessed by indigenous fluorescence, as seen with SYBR Gold (Fig. 5C, F); 3) MF10S is more sensitive than FRET because the optics of a confocal microscope are used; 4) problems due to air bubbles as seen with the FRET system are avoided because the MF10S system allows fluorescent signals to come from a small volume element (10^{-15} l); and 5) the time required for analysis is much shorter compared with the PAGE-radioisotope system that is often accompanied by a degradation of compounds.

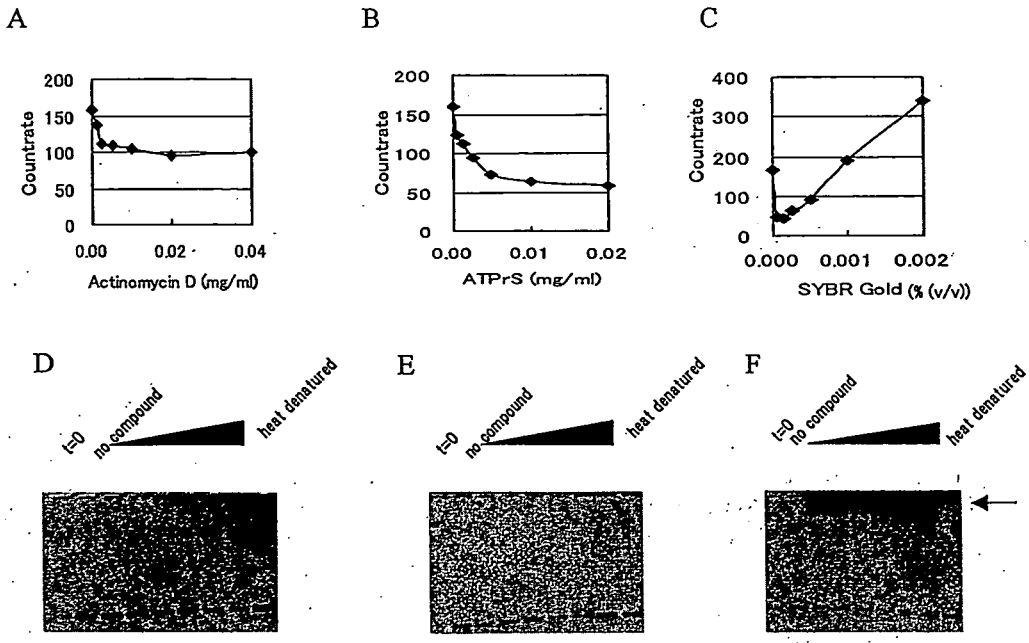

Fig. 5. Inhibition of Werner Helicase Activity by Actinomycin D (A), ATPγS (B) and SYBR Gold (C)

The inhibition was measured using the MF10S. The same samples were also analyzed by PAGE: actinomycin D (D), ATPγS (E) and SYBR Gold (F). The strong fluorescent band near the wells in F is due to the fluorescence of SYBR Gold itself which is also reflected in the increase in the countrate at higher doses in C.

The MF10S system has the potential to screen anti-cancer drugs. First, because the down-regulation of WRN helicase is expected to cause an increase in the sensitivity of dominant negatively expressed cell lines against 4NQO.[19] Second, because the MF10S system described in this paper could also monitor the inhibitory effect of adriamycin (data not shown) that has an intercalating activity and is used as an anti-tumor drug.[20,21]

Acknowledgements We thank Mr. Kazuhito Gohda, Genome Medical Business Division, Olympus Optical Co., Ltd. for his help in the assay using the MF10S single-molecule fluorescence detection system, and Dr. Masanobu Sugimoto of GeneCare Research Institute Co., Ltd. for his invaluable discussion and help to prepare this manuscript.

REFERENCES

1) Borowski P., Niebuhr A., Schmitz H., Hosmane R. S., Bretner M., Siwecka M. A., Kulikowski T., *Acta Biochimica Polonica*, **49**, 597—614 (2002).
2) Crute J. J., Grygon C. A., Hargrave K. D., Simoneau B., Faucher A.-M., Bolger G., Kibler P., Liuzzi M., Cordingley M. G., *Nature Medicine*, **8**, 386—391 (2002).
3) Kleymann G., Fischer R., Betz U. A. K., Hendrix M., Bender W., Schnetder U., Handke G., Eckenberg P., Hewlett G., Pevzner V., Baumeister J., Weber O., Henninger K., Keldenich J., Jensen A., Kolb J., Bach U., Popp A., Maben J., Frappa I., Haebich D., Lockhoff O., Rubsamen-Waigmann H., *Nature Medicine*, **8**, 392—398 (2002).
4) Faucher A. M., White P. W., Brochu C., Grand-Maitre C., Rancourt J., Fazal G., *J. Med. Chem.*, **47**, 18—21 (2004).
5) Yu C. E., Oshima J., Fu Y. H., Wijsman E. M., Hisama F., Alisch R., Matthews S., Nakura J., Miki T., Ouais S., Martin G. M., Mulligan J., Schellenberg G. D., *Science*, **272**, 258—262 (1996).
6) Shimamoto A., Sugimoto M., Furuichi Y., *Int. J. Clin. Oncol.*, **9**, 288—298 (2004).
7) Okada M., Goto M., Furuichi Y., Sugimoto M., *Biol. Pharm. Bull.*, **21**, 235—239 (1998).
8) Stryer L., Haugland R. P., *Proc. Natl. Acad. Sci. U.S.A.*, **58**, 719—726 (1967).
9) Parkhurst K. M., Parkhurst L. J., *Biochemistry*, **34**, 293—300 (1995).
10) Parkhurst K. M., Parkhurst L. J., *Biochemistry*, **34**, 285—292 (1995).
11) Suzuki N., Shimamoto A., Imamura O., Kuromitsu J., Kitao S., Goto M., Furuichi Y., *Nucleic Acids Res.*, **25**, 2973—2978 (1997).
12) Kato N., Okamoto N., Kobayashi S., Otsuka C., Nagano T., *Idenshigaku*, **6**, 271—277 (2002) (in Japanese).
13) Lohman T. M., Bjornson K. P., *Ann. Rev. Biochem.*, **65**, 169—214 (1996).
14) Houston P., Kodadek T., *Proc. Natl. Acad. Sci. U.S.A.*, **91**, 5471—5474 (1994).
15) Choudhary S., Sommers J. A., Brosh R. M., Jr., *J. Biol. Chem.*, **279**, 34603—34613 (2004).
16) Haupts U., Rudiger M., Ashman S., Turconi S., Bingham R., Wharton C., Hutchinson J., Carey C., Moore K. J., Pope A. J., *J. Biomolecular Screen.*, **8**, 19—33 (2003).
17) Jager S., Brand L., Eggeling C., *Curr. Pharm. Biotechnol.*, **4**, 463—476 (2003).
18) Earnshaw D. L., Moore K. J., Greenwood C. J., Djaballah H., Jurewicz A. J., Murray K. J., Pope A. J., *J. Biomolecular Screen.*, **4**, 329—247 (1999).
19) Bai Y., Murnane J. P., *Hum. Genet.*, **113**, 337—347 (2003).
20) Kanter P. M., Schwartz H. S., *Leuk Res.*, **3**, 277—283 (1979).
21) Cullinane C., Cutts S., Panousis M. C., Phillips D. R., *Nucleic Acids Res.*, **28**, 1019—1012 (2000).

Gene Transfer to Corneal Epithelium and Keratocytes Mediated by Ultrasound with Microbubbles

Shozo Sonoda,[1] Katsuro Tachibana,[2] Eisuke Uchino,[1] Akiko Okubo,[1] Matsuo Yamamoto,[3] Kenji Sakoda,[4] Toshio Hisatomi,[5] Koh-Hei Sonoda,[5] Yoichi Negishi,[6] Yuichi Izumi,[4] Sonshin Takao,[7] and Taiji Sakamoto[1]

PURPOSE. The cornea is an ideal organ for evaluating gene transfer because it can be treated noninvasively and monitored easily. The present study was performed to investigate the practical efficacy and safety of ultrasound (US) plus microbubble (MB)–mediated gene transfer to cornea.

METHODS. Cultured rabbit corneal epithelial (RC-1) cells were incubated in 24-well dishes with plasmid DNA having a green fluorescent protein (GFP) gene under a cytomegalovirus promoter. The cells were exposed to US under different intensities (1 MHz; power, 0.5~2 W/cm^2; duration, 15–120 seconds; duty cycle, 20%–100%). The effect of simultaneous stimulation with MBs was also examined. Gene transfer was quantified by counting the number of GFP-positive cells under microscopy. Furthermore, in vivo gene transfer was examined by GFP plasmid injection into rabbit cornea and US exposure with MBs.

RESULTS. In the in vitro study, DNA exposure alone could not transfer gene into cultured RC-1 cells; US enhanced gene transfer slightly. Coexposure with MBs significantly increased gene transfer efficiency. In the in vivo study, DNA injection alone could transfer the gene to a limited degree, but plasmid injection plus US with MBs strongly increased gene transfer efficiency without apparent tissue damage, and gene transfer was achieved two dimensionally.

CONCLUSIONS. US with MBs greatly increases gene transfer to in vivo and in vitro corneal cells. This noninvasive gene transfer method may be a useful tool for clinical gene therapy. (*Invest Ophthalmol Vis Sci.* 2006;47:558–564) DOI:10.1167/iovs.05-0889

A modality to efficiently deliver genes to living tissue is essential for gene therapy and genetic research. The basic technology of gene delivery can be divided into two categories, a virus vector–mediated method and a non–virus vector–mediated method.[1–3] The virus vector–mediated method can transfer the gene of interest with high efficiency, but concern about safety issues prevents clinical application for common diseases.[3–5] The non–virus vector–mediated method is comparatively safe, but gene transfer efficiency does not reach a satisfactory level.[6–9] Among these methods, the mechanical enhancing method is unique because it is free from a biochemical agent that has not been proven to be safe for humans; thus, clinical application might be more easily accepted. Electroporation can be used for this purpose but often results in severe cell damage.[10,11] In contrast, it recently became apparent that ultrasound (US) can enhance gene transfer to mammalian cells in vitro and in vivo without cell damage,[12–16] and US-mediated gene therapy has been reported in vessels and muscles of animal studies.[17,18] US is now widely used for clinical examinations and therapies, and its safety has been reliably established.

The cornea plays an important role in maintaining vision. Vision can be seriously impaired as a result of corneal cloudiness caused by insufficient wound healing or by the metabolic processes of cornea. Although corneal surgery is widely performed and may be performed even more often as more refractive surgery is performed, the cellular and molecular events that control wound healing within the corneal stroma are not well understood.[19,20] The cornea is an external tissue suitable for gene therapy because of its easy accessibility by surgical maneuvers, including US. In addition, gene transfer can be easily monitored by noninvasive methods such as microscopic observation.[21]

Microbubbles (MBs), which are gas bubbles measuring approximately 3 μm in diameter, have been developed mainly as contrast agents to improve ultrasonographic images. They have shown promise in gene therapy for several reasons. MBs act as cavitation nuclei, effectively focusing ultrasound energy, and they can potentiate bioeffects. Evidence indicates that the ultrasound energy needed can be greatly reduced; therefore, the lower power used in diagnostic imaging systems may be sufficient to produce therapeutic effects.[22–24]

Simultaneous use of US and MBs has been found to increase gene transfer efficiency.[25–32] However, to our knowledge, few reports have been published of detailed analyses of US-mediated gene transfer with MBs. In this study, we performed a detailed analysis of gene transfer mediated by US with MBs using cornea, and we show two-dimensional gene transfer achieved by this method.

METHODS

In Vitro Study

Cell Culture. Rabbit corneal epithelial (RC-1) cells (JCRB0246) were obtained from Human Science Research Resource Bank (Tokyo, Japan) and incubated in modified Eagles medium (MEM; Sigma-Aldrich, St. Louis, MO) with 10% fetal bovine serum (FBS; Invitrogen-Gibco, Grand Island, NY) and streptomycin/penicillin (Wako, Osaka, Japan). All cells used in the studies were from passages 4 to 6.

From the Departments of [1]Ophthalmology and [4]Periodontology and the [7]Research Center for Life Science Resources, Kagoshima University, Kagoshima, Japan; the [2]Department of Anatomy, Fukuoka University School of Medicine, Fukuoka, Japan; the [3]Department of Periodontology, Showa University School of Dentistry, Tokyo, Japan; the [5]Department of Ophthalmology, Graduate School of Medical Sciences, Kyushu University, Fukuoka, Japan; and the [6]School of Pharmacy, Tokyo University of Pharmacy and Life Sciences, Tokyo, Japan.

Supported by Grants-in-Aid for Scientific Research (17390469 and 14370560) and Grant-in-Aid for Young Scientists (16791056) from the Ministry of Education, Science and Culture of the Japanese Government.

Submitted for publication July 11, 2005; revised September 9, 2005; accepted December 22, 2005.

Disclosure: **S. Sonoda**, None; **K. Tachibana**, None; **E. Uchino**, None; **A. Okubo**, None; **M. Yamamoto**, None; **K. Sakoda**, None; **T. Hisatomi**, None; **K.-H. Sonoda**, None; **Y. Negishi**, None; **Y. Izumi**, None; **S. Takao**, None; **T. Sakamoto**, None

The publication costs of this article were defrayed in part by page charge payment. This article must therefore be marked "*advertisement*" in accordance with 18 U.S.C. §1734 solely to indicate this fact.

Corresponding author: Taiji Sakamoto, Department of Ophthalmology, Kagoshima University Faculty of Medicine, 8-35-1 Sakuragaoka, Kagoshima, Japan 890-8520; tsakamot@m3.kufm.kagoshima-u.ac.jp.

Investigative Ophthalmology & Visual Science, February 2006, Vol. 47, No. 2

Plasmids. An expression vector for the green fluorescent protein (GFP) gene, *pEGFP-N2*, a mammalian expression vector containing a cytomegalovirus immediate-early enhancer/promoter, was obtained from Clontech Co., Ltd. (Palo Alto, CA). Plasmids grown in *Escherichia coli* host strain XLI-blue were purified (Plasmid Kit; Qiagen, Valencia, CA) and suspended in TE buffer (pH 8.0) at a concentration of 1.0 μg/μL. Plasmids were then suspended in phosphate-buffered saline (PBS; Invitrogen-Gibco), and the pH was adjusted to 7.35.

Ultrasound Exposure. RC-1 cells were collected with trypsin (Sigma-Aldrich), passed through a cell strainer (Becton Dickinson, Franklin Lakes, NJ), and put into a 48-well collagen type 1-coated glass bottom chamber (Asahi Technoglass, Chiba, Japan) filled with 400 μL MEM with 10% FBS, 4×10^4cells/well. A plasmid solution 0.5 μL was added to the medium. Immediately thereafter, US was exposed to the medium using a 6-mm probe generated by an US machine (Sonitron 2000; Richmar, Inola, OK). During exposure, the medium-containing cells were gently stirred by a magnetic stirrer (300 rpm). To induce MBs, perflutren protein type A microsphere (Optison; Amersham Health, Princeton, NJ)—a well-established, second-generation US medical diagnostic product with robust capability—was used. It is an albumin-shelled US contrast agent composed of approximately 5 to 8×10^8 MBs per milliliter measuring between 2 and 4.5 μm in diameter and filled with octaperfluoropropane. The indicated percentage was added to the plasmid solution (0.5, 0.25, or 0.1 μL), gently mixed, and left for 60 seconds. Immediately thereafter, the mixed solution was added to the dish and exposed to US as described.

Gene Transfer Efficiency. After gene transfer treatment, including plasmid alone or plasmid plus US exposure, the cells were incubated in a medium containing 10% FBS for 48 hours and then were observed by phase-contrast microscopy with or without a 515-nm filter (Olympus, Tokyo, Japan). A randomly selected field (4 fields/well with 100 × magnification) was photographed. The photographs were monitored by a NIH image analyzer, and the ratio of GFP-positive cells to all cells in each field was evaluated by masked observers. To determine the duration of GFP expression, GFP expression was evaluated on days 4, 8, 14, and 30.

Cell Survival and Cell Damage. Survival of cells was evaluated by counting living cells. Briefly, after 48 hours of incubation, the dishes were washed twice with PBS, four microscopic fields per well were photographed, and the living cells were counted. Cell damage was evaluated by lactate dehydrogenase (LDH)-releasing assay according as the manufacturer's instructions (Roche, Penzberg, Germany). Cells cultured on a 48-well plate were treated by each procedure, and cell damage was evaluated after 6 hours. The most severe cell damage was obtained by treatment with 1% Triton X (Sigma-Aldrich) and was used as a positive control. Cells with no treatment were applied as negative controls. Cell damage was expressed as: % LDH of sample − LDH of negative control/LDH of positive control − LDH of negative control.

In Vivo Study

After obtaining the approval of Kagoshima University ethics committee, all animals were used humanely in strict compliance with the ARVO Statement for the Use of Animals in Ophthalmic and Vision Research.

New Zealand albino rabbits (male; age, 14 weeks; weight, 3000 g; KBT Oriental Co., Saga, Japan) were first anesthetized with intramuscular injection of ketamine hydrochloride (14 mg/kg) and xylazine hydrochloride (14 mg/kg). Plasmid 10 μL mixed with PBS 2 μL was injected under surgical microscopy into the center of each cornea using a syringe with a 30-gauge needle. Immediately thereafter, a 6-mm US probe was placed directly on the corneal surface, and US was generated. When MBs were used, plasmid 10 μL mixed with perflutren protein (Optison; Amersham Health) 2 μL was injected instead of a plasmid with PBS. The intensity of US was set at 1 MHz, 120 seconds, 50% duty cycle, and 3 US powers—1 W/cm^2, 1.5 W/cm^2, and 2 W/cm^2—were examined.

GFP Expression. The presence of fluorescence signaling in the in vivo gene expression was determined using direct stereomicroscopy 72 hours after gene transfer (Olympus, Tokyo, Japan). The value of gene transfer was graded according to our scoring system by 3 masked observers. Only GFP expression scores agreed to by at least 2 of the observers were used in the analysis. Scoring criteria and representative photographs are shown in Figure 1. Transfection efficiency was expressed by a score of 0 to 5 (0 = not GFP positive; 5 = most intensely GFP positive).

Histology. All the animals were killed by overdose intravenous injection of pentobarbital. The eyes were enucleated 48 hours after treatment and were immediately frozen in liquid N2-cooled isopentane. Serial sections (6 μm) were sliced with a cryostat, placed on slides, and air dried. Regular fluorescent images and differential interference images were obtained by fluorescence microscopy (BX-FLA; Olympus, Tokyo, Japan) and were fitted using the IP Laboratory program (Scanalytics, Inc.; Fairfax, VA) on a personal computer. For light microscopy, the eyes were fixed with 3.7% formaldehyde in PBS, dehydrated with a graded alcohol series, and embedded in paraffin. Sections were cut and stained with hematoxylin and eosin. For the electron microscopy, the tissue was fixed with 4% paraformaldehyde, and the specimens were then dehydrated in a series of graded ethanols and embedded in epoxy resin. Thin sections were cut on an ultramicrotome, stained with uranyl acetate-lead citrate, and observed with an electron microscope (JEM-100CX; JEOL, Tokyo, Japan), as described. All the specimens were then observed by 2 masked observers who received no information about the specimens.

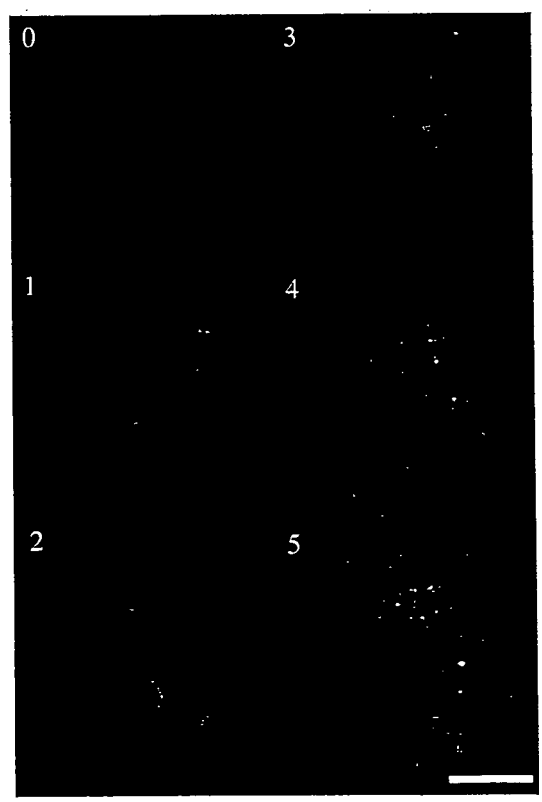

FIGURE 1. Representative photographs of scoring criteria. Gene transfer efficiency was expressed as a score of 0 to 5. Scoring was performed by 3 masked observers according to the following criteria. 0: no positive cells; 1: 1 to 25 positive cells in each field; 2: 26 to 50 positive cells in each field; 3: 51 to 75 positive cells in each field; 4: 75 to 150 positive cells in each field; 5: 151 or more positive cells in each field. Bar, 400 μm.

Statistical Analysis

All values were expressed as mean ± SEM. Analysis of variance with subsequent Scheffe test and Mann-Whitney *U* test was used to determine the significance of the difference in multiple comparison. Differences with a $P < 0.05$ were considered significant.

Results

In Vitro Study

Gene Transfer by Ultrasound. Numerous RC-1 cells were GFP positive after US exposure with the plasmid solution (Fig. 2A). Cells treated with the plasmid solution alone or the plasmid solution with MB perflutren protein (Optison; Amersham Health) alone did not show any fluorescein (Fig. 2B).

Gene Transfer by US Plus MBs. Under any of the following experimental US conditions—1 W/cm^2, 60 seconds, duty cycle 50%; 1 W/cm^2, 120 seconds, duty cycle 50%; 2 W/cm^2, 60 seconds, duty cycle 50%; 2 W/cm^2, 120 seconds, duty cycle 50%—the ratio of GFP-positive cells treated by US with MBs was significantly (two to four times) higher than that by US alone (Mann-Whitney *U* test, $P < 0.01$ Fig. 2C). To identify the optimal conditions to transfer genes by US plus MBs, the following four parameters were examined.

Duty Cycle. According to our previous studies, three duty cycles (20%, 50%, or 100%) were examined under an intensity of 1 W/cm^2 and 60-second exposure with 20% MBs.[29,30,32] As a result, the GFP-positive cell ratios were 11.3% with a duty cycle of 20%, 18.0% with a duty cycle of 50%, and 35.6% with a duty cycle of 100%. The GFP-positive cell ratio of duty cycle 100% US plus MBs was significantly higher than that under the other three conditions (Scheffe test, $P < 0.01$; Fig. 3A). On the other hand, the average number of survival cells was low with a duty cycle of 100%; for 79 cells per field, the duty cycle was 20%; for 171 cells per field, it was 50%; for 17.1 cells per field per, it was 100%. Cell damage was high in US, with a duty cycle of 20% or 100% in LDH assay (Fig. 3B). These results indicate that a duty cycle of 50% is preferable for obtaining high gene transfer efficiency with minimal cell damage.

MBs. Three concentrations of MBs—20%, 50%, and 100%—were examined under the US condition of 1 W/cm^2, 60 seconds, and duty cycle 50%. The GFP-positive ratio was highest in cells treated by US with 20% MBs (Scheffe test, $P < 0.01$; Fig. 3C). Cell survival was lowest in the 100% MB group, and no significant difference was found between the 20% and the 50% MB groups (170.7 cells/field in 20% MBs, 163 cells/field in 50% MBs, 38 cells/field in 100% MBs). A similar tendency was found by LDH assay (data not shown). Thus, 20% MBs was preferable.

Exposure Time. According to our previous study, a US exposure duration exceeding 120 seconds significantly damaged cells[29,32]; thus, a US exposure time of 15 to 120 seconds was examined under the condition of 1 W/cm^2, duty cycle 50%, with 20% MBs. As a result, the GFP-positive ratio was equally high for 60-and 120-second exposures (Fig. 3D). Cell damage was not apparent in any experimental group (Fig. 3E).

US Intensity. US intensities of 0.5, 1.0, 1.5, and 2.0 W/cm^2 were examined under the condition of 50% duty cycle and 60-second exposure with 20% MBs. A GFP-positive ratio of 0.5 W/cm^2 US group was significantly smaller than that in any of the other 3 groups (Scheffe test, $P < 0.01$; Fig. 2F). LDH assay also indicated that cell damage was significantly high in the 1.5 and 2.0 W/cm^2 exposure groups ($P < 0.01$; Fig. 3G), whereas little cell damage was observed in cells treated with 0.5 or 1.0 W/cm^2 US intensity. Representative images are shown in Figures 3H and 3I.

In Vivo Study

Gene Transfer by US. All GFP-positive cells in rabbit eyes underwent treatment. Eyes that received plasmid injection alone showed mild GFP-positive cells distributed within the injected area. GFP-positive cells were observed mainly in the corneal stroma. Average fluorescein score was 2.1 ($n = 24$). On the other hand, eyes that received plasmid injection and US (1 W/cm^2, 120 seconds, duty cycle 50%) had more GFP-positive cells (average score, 2.6; $n = 14$) than those that received plasmid injection alone. However, the difference was not statistically significant (Fig. 4).

Gene Transfer by US and MBs. From the in vitro study, 20% MBs were chosen. The average score of GFP-positive cells in cornea was 3.5 for eyes treated by US of 1 W/cm^2, 120 seconds, 50% duty cycle with MBs ($n = 41$). A significantly higher score (4.5) was obtained with simultaneous treatment by US and MBs than by US alone (2.6) or MBs alone (2.0) (Scheffe test, $P < 0.05$; Fig. 4), and it was achieved with US of 2 W/cm^2, 120 seconds, and 50% duty cycle ($n = 12$). GFP-

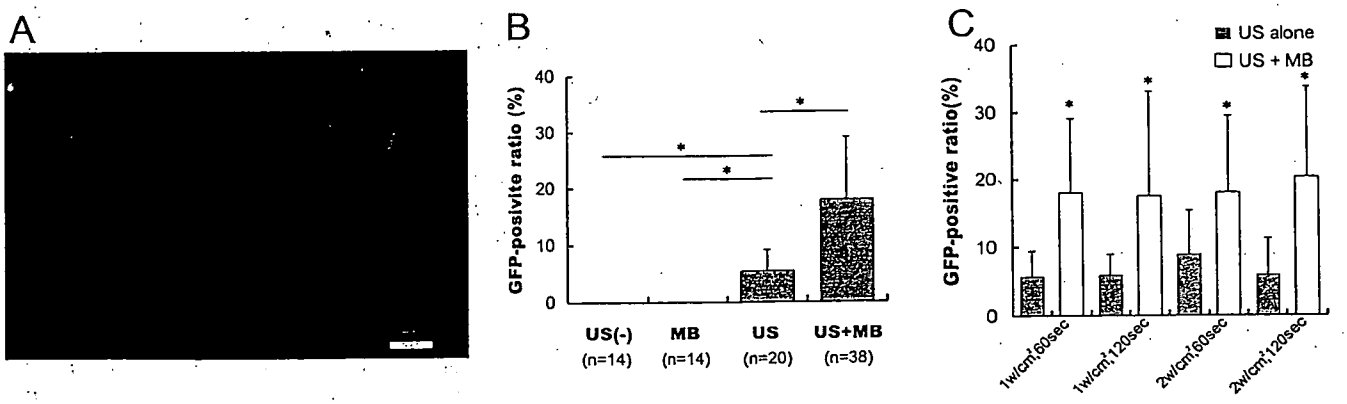

FIGURE 2. GFP-positive cells in gene-transferred rabbit corneal epithelial (RC-1) cells. (A) Fluorescence photograph of gene-transferred RC-1 cells. Many cells show a GFP-positive reaction in the whole cytoplasm. Bar, 100 μm. (B) GFP-positive ratio by different methods. Numerous RC-1 cells were GFP positive after ultrasonic exposure with the plasmid solution. Cells treated with the plasmid solution alone or the plasmid solution with perflutren protein (Optison; Amersham Health) alone did not show any fluorescein (Mann-Whitney *U* test, $^*P < 0.01$). (C) GFP-positive ratio of cells treated by US exposure with MBs. GFP-positive ratio treated by US with MBs was significantly higher (2–4 times) than that by US alone (Mann-Whitney *U* test, $^*P < 0.01$). 1 W/cm^2, 60 seconds, duty cycle 50%: US only, $n = 14$; with MB, $n = 38$. 1 W/cm^2, 120 seconds, duty cycle 50%: US only, $n = 15$; with MB, $n = 24$. 2 W/cm^2, 60 seconds, duty cycle 50%: US only, $n = 15$; with MB, $n = 23$. 2 W/cm^2, 120 seconds, duty cycle 50%: US only, $n = 15$; with MB, $n = 13$.

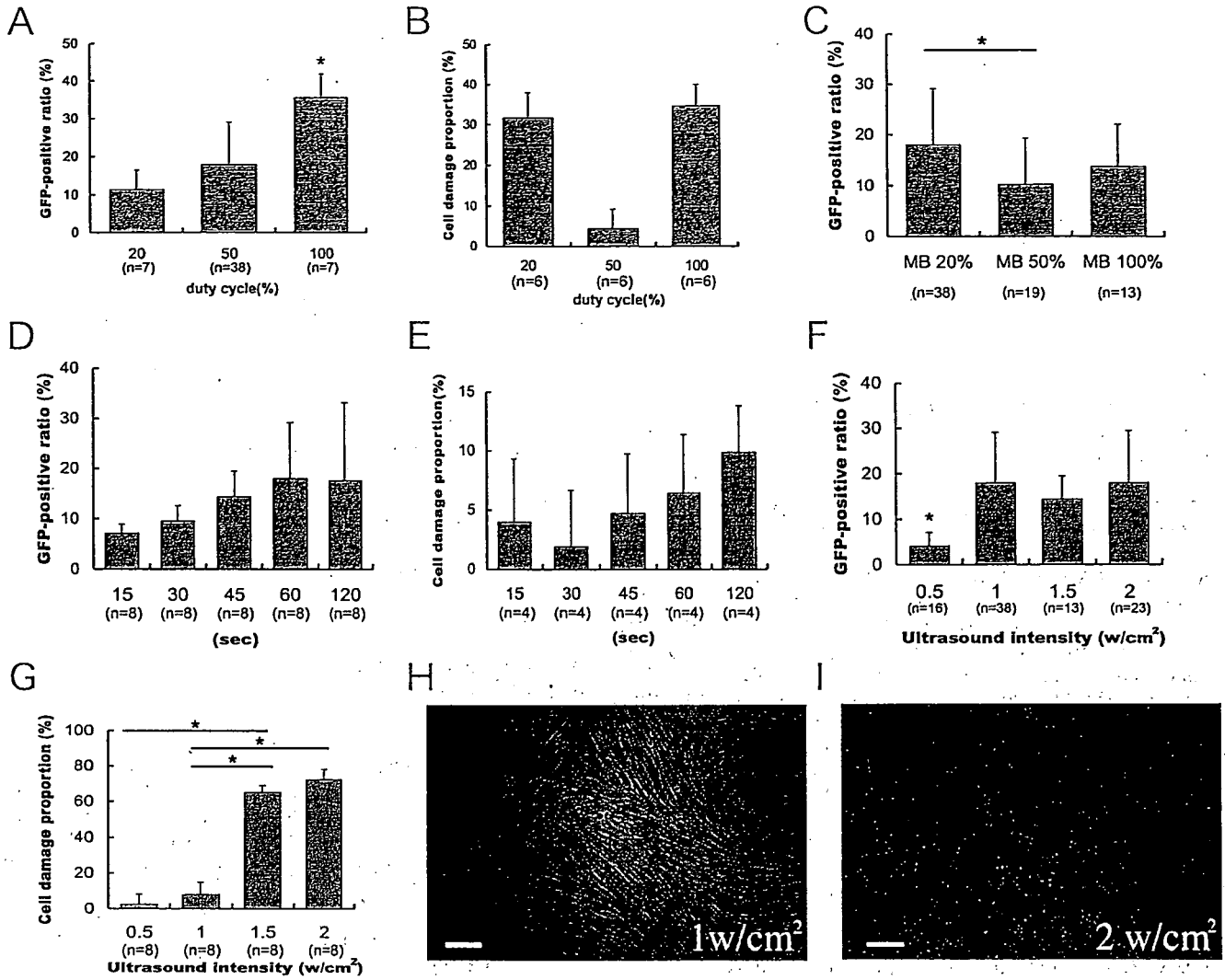

FIGURE 3. Gene transfer by US and MBs under different conditions. (A) GFP-positive ratio at a different duty cycle. GFP-positive ratio of duty cycle 100% US plus MBs was significantly higher than under the other 3 conditions (Scheffe test, $^*P < 0.01$). (B) Cell damage at different duty cycle. LDH assay indicates that cell damage was high in US at duty cycle 20% or 100%. (C) GFP-positive ratio at different concentrations of MBs. GFP-positive ratio was highest in cells treated by US with 20% MBs (Scheffe test, $^*P < 0.01$). (D) GFP-positive ratio at different US exposure times. GFP-positive ratio was equally high at 60- and 120-second exposures. (E) Cell damage at different US exposure times. Cell damage was not apparent in any experimental group. (F) GFP-positive ratio at different US powers. GFP-positive ratio of 0.5 W/cm^2 US group was significantly smaller than that of any of the other 3 groups (Scheffe test, $^*P < 0.01$). (G) Cell damage at different US powers. LDH assay indicates that cell damage was significantly high in the 1.5 or 2.0 W/cm^2 exposure group ($^*P < 0.01$), whereas little cell damage was noticed in cells treated with 0.5 or 1.0 W/cm^2 US power. (H) Phase-contrast photograph of RC-1 cells immediately after US exposure. No apparent cell damage was observed. Bar, 100 μm. (I) Phase-contrast photograph of RC-1 cells immediately after US exposure. Apparent cell damage was found in many cells (*arrows*). Bar, 100 μm.

positive cells were observed exclusively where US was exposed (Fig. 5). US intensity greater than 3 W/cm^2 caused immediate stromal haziness, which resolved spontaneously with no treatment (data not shown).

Duration of GFP Expression. The duration of GFP expression in cornea was evaluated in the eye treated with US and MBs under 20% MBs, 2 W/cm^2, 120 seconds, duty cycle 50%. GFP-positive cells appeared on the following day and increased the strength and the number of GFP-positive cells for 8 days (Fig. 6). GFP-positive cells in cornea gradually decreased in number and strength over time, and the average GFP-positive score on day 14 was 2 ($n = 13$) (Scheffe test $P < 0.01$). On day 30, only a faint GFP-positive reaction was noticed ($n = 4$).

Histologic Findings. Fluorescence microscopic examination showed that GFP was present in spindle-shaped cells in the targeted regions of the corneal stroma; thus, we speculated that keratocytes were also present (Fig. 7). Importantly GFP-positive cells were limited to the US-exposed area. No GFP was detected in untreated cornea or other intraocular tissues, such as ciliary epithelial cells, trabecular meshwork, cells lining Schlemm canal, lens epithelial cells, or retina (data not shown). Light and electron microscopic examination 48 hours after treatment showed no corneal damage, such as opacity or persistent epithelial defects, after US plus MB treatment, even under the strongest power studied in this series (2 W/cm^2, 120 seconds, duty cycle 100%; data not shown).

DISCUSSION

US is broadly used for clinical imaging, and its safety has been reliably established. Only in the past few years have studies demonstrated US-enhanced gene delivery to mammalian cells in vitro and in vivo.[12–18] Moreover, the presence of MBs near

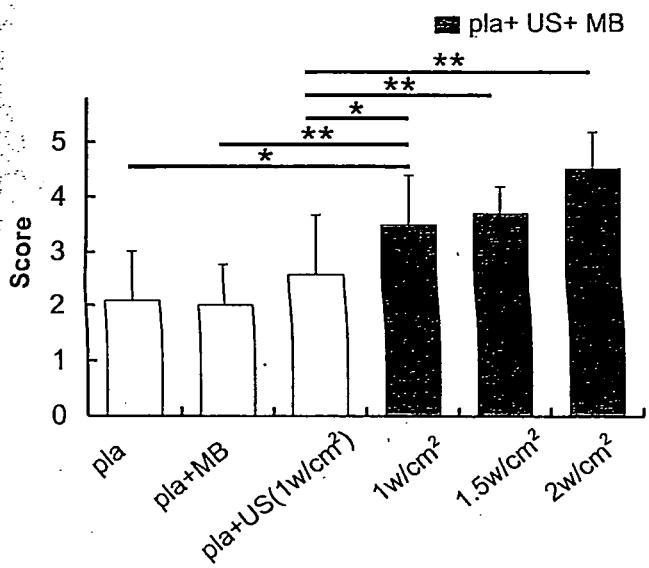

FIGURE 4. Gene transfer to rabbit cornea in vivo by US or MBs. Eyes that received plasmid injection alone or plasmid with MBs showed fluorescein-positive cells widely distributed within the injected area (plasmid alone, $n = 24$; plasmid with MB, $n = 8$). Eyes that received plasmid injection and US showed more numerous GFP-positive cells ($n = 14$) than those that received plasmid injection alone. A significantly higher score was obtained by simultaneous treatment of US and MBs (1 W/cm², $n = 41$; 1.5 W/cm², $n = 13$; 2 W/cm², $n = 12$) than by US alone (2.6) or MBs alone (2.0) (Scheffe test, $^*P < 0.05$, $^{**}P < 0.01$). Pla, plasmid DNA injection.

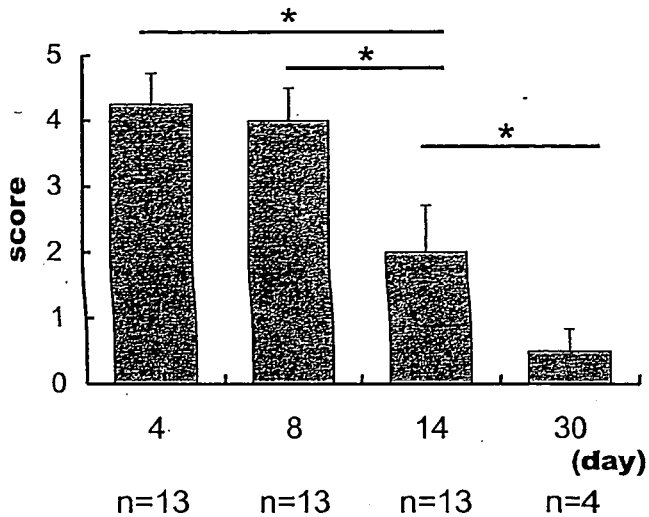

FIGURE 6. Duration of GFP expression in rabbit cornea was evaluated in the eye treated with US and MBs. GFP-positive cells appeared on the following day and increased the strength and number of GFP-positive cells for 8 days. GFP-positive cells in cornea gradually decreased in number and strength over time, and the average GFP-positive score on day 14 was 2 ($n = 13$) (Scheffe test, $^*P < 0.01$). On day 30, only faint GFP-positive reaction was observed ($n = 4$).

the cells further increases the gene transfection rate by lowering the acoustic pressure threshold needed to induce the microjets that penetrate the cellular membrane.[25-32] Sonography contrast-agent MBs with diameters ranging from 1 to 10 μm are considered ideal for this purpose. To gain further insight into the practicability of sonoporation, the cornea was selected as the subject of the present study because it can be noninvasively treated and monitored with the use of standard ophthalmological equipment, allowing visualization the cornea and the surrounding tissues under high magnification and per-

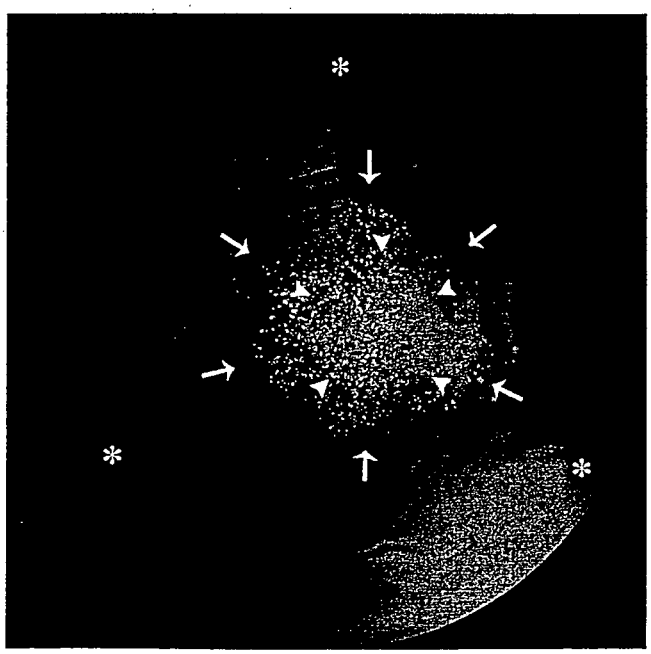

FIGURE 5. Fluorescence photograph of rabbit cornea 7 days after treatment. Twelve microliters plasmid with MBs was injected into the central cornea (*arrows*); this was followed by US exposure. *Arrowheads* indicate exactly where the US probe was placed. GFP-positive cells were specifically located where the US was exposed. A few GFP-positive cells are seen in the surrounding area. *Asterisks* indicate the corneal margin.

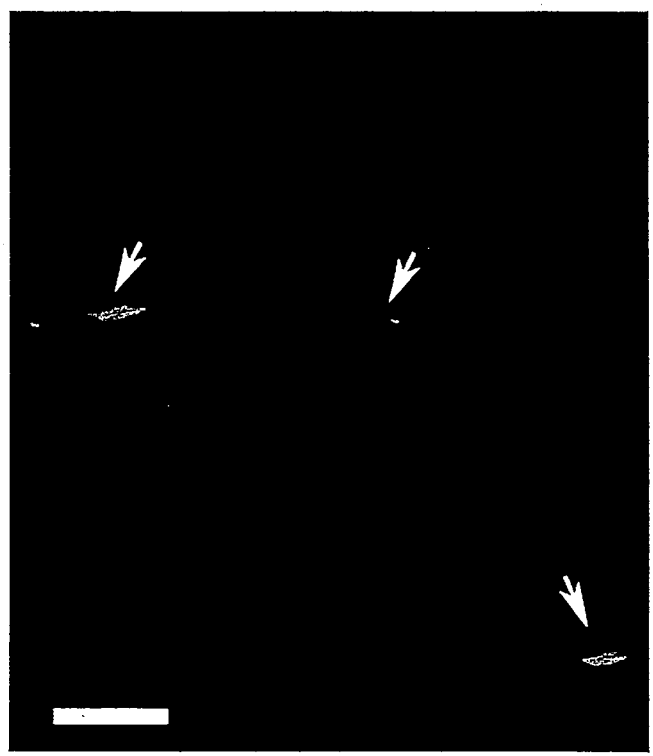

FIGURE 7. Fluorescence microscope photograph of rabbit cornea after treatment with US and MBs (2 W/cm², duty cycle 50%, 120 seconds). GFP is present mainly in spindle-shaped cells in the targeted regions of the corneal stroma (*arrows*). Bar, 10 μm.